

## The implications of K-Ar glauconite dating of the Diest Formation on the paleogeography of the Upper Miocene in Belgium.

Noël VANDENBERGHE<sup>1</sup>, W. Burleigh HARRIS<sup>2</sup>, J.M. WAMPLER<sup>3</sup>, Rik HOUTHUYS<sup>4</sup>, Stephen LOUWYE<sup>5</sup>, Rieko ADRIAENS<sup>1</sup>, Koen VOS<sup>1</sup>, Timothy LANCKACKER<sup>6</sup>, Johan MATTHIJS<sup>6</sup>, Jef DECKERS<sup>6</sup>, Jasper VERHAEGEN<sup>1</sup>, Piet LAGA<sup>7</sup>, Wim WESTERHOFF<sup>8</sup> & Dirk MUNSTERMAN<sup>8</sup>

<sup>1</sup> Department Earth and Environmental Sciences, Katholieke Universiteit, Leuven, Belgium.

E-mail: Noel.Vandenberghe@ees.kuleuven.be

<sup>2</sup> North Carolina Geological Survey, MSC 1620, Raleigh, NC 27699, USA. E-mail: harrisw@uncw.edu

<sup>3</sup> Department of Geosciences, Georgia State University, Atlanta, GA 30303, USA. E-mail: claylab@gsu.edu

<sup>4</sup> Geoconsultant, Halle, Belgium. E-mail: rik.houthuys@telenet.be

<sup>5</sup> Research Unit Palaeontology, Ghent University, Belgium. E-mail: Stephen.Louwye@UGent.be

<sup>6</sup> VITO, Flemish Institute for Technological Research, Mol, Belgium. E-mail: jef.deckers@vito.be

<sup>7</sup> Belgian Geological Survey, Brussels, Belgium. E-mail: Piet.laga@skynet.be

<sup>8</sup> Geological Survey of the Netherlands-TNO, Utrecht, the Netherlands. E-mail: dirk.munsterman@tno.nl; wim.westerhoff@tno.nl

**ABSTRACT.** The glauconite-rich Diest Formation in central and north Belgium contains sands in the Campine subsurface and the hilly Hageland area that can be distinguished from each other. The Hageland Diest Sands member contains no stratigraphically relevant fossils while in the Campine subsurface dinoflagellate cysts are common and show a stratigraphic range covering the entire Tortonian stage. K-Ar dates were determined for glauconite from 13 selected samples spread over both areas. A glauconite date corresponding to the earliest Tortonian indicates newly formed glauconite was incorporated into a greensand at the base of the Diest Formation in the central Campine area. All other dates point at reworked glauconite and can be organized in two groups, one reflecting a Burdigalian age and another reflecting a Langhian age. These data and the thickness and glauconite content of the Diest Formation imply massive reworking of older Miocene deposits.

The paleogeographic implications of these data lead to the tentative recognition of two Tortonian sedimentary sequences. An older one corresponding to dinoflagellate biochron DN8 comprises the Deurne Member, part of the Dessel Member, the Hageland Diest member, the eastern Campine Diest member and some basal sands of the Diest Formation in the central Campine. A younger sequence corresponding to dinoflagellate biochrons DN9 and 10 was strongly influenced by the prograding proto-Rhine delta front in the Roer Valley Graben to the northeast. The subsiding Campine basin was filled from east to west during this second cycle.

**KEYWORDS:** Glauconite reworking, Tortonian, Campine, Hageland, paleogeography

### 1. Introduction

The Diest Formation is a glauconite-rich upper Miocene (Tortonian) sand unit with a maximum thickness of circa 100 m (Vandenberghe et al., 1998). The formation consists of the Deurne and Dessel Members at the base, considered laterally equivalent deposits, and the proper Diest member at the top (Table 1). The formation crops out in central Belgium where its top is cemented by limonite, which accounts for the typical Hageland region hilly geomorphology. The Diest member occurs also at relatively shallow depths in the subsurface of the Campine area where it is covered by the slightly younger glauconitic Kasterlee Formation of Messinian age and also by Pliocene and Pleistocene sediments (Gulinck, 1962). The lithostratigraphic units referred to in the text

are shown in Table 1 and the geographical locations are indicated on Fig. 1.

Arguments are developed in this paper to differentiate the Diest Sands in the Hageland area from those in the Campine area. Glauconite dates were obtained in a search to support this differentiation. The inferred sources and estimated ages of the Diest Sands in the different areas and the implications for the late Serravallian and Tortonian paleogeography are discussed.

### 2. The geological setting and the stratigraphic position of the Diest Formation

The Diest Formation in the Hageland shows an unconformable relationship with the older strata on a geological map. It trends

|                                |                   | Antwerp area       | Antwerp Campine | Hageland area       | Limburg Campine  |                   |                      | Roer Valley Graben   |
|--------------------------------|-------------------|--------------------|-----------------|---------------------|------------------|-------------------|----------------------|----------------------|
| Upper<br>Miocene               |                   |                    |                 | Kasterlee Formation |                  |                   |                      | Breda Formation      |
|                                | Diest Formation   | no deposits        | Poppel facies   |                     |                  | Gruithrode facies | Diest Formation      |                      |
|                                |                   |                    | Diest member    |                     |                  | Opoeteren facies  |                      |                      |
|                                |                   |                    | Dessel Member   |                     |                  |                   |                      |                      |
|                                |                   | Deurne Member      |                 |                     |                  |                   |                      |                      |
| Lower and<br>Middle<br>Miocene | Berchem Formation | Zonderschot facies |                 |                     | Opgrimbie facies |                   | Bolderberg Formation | Vrijherenberg Member |
|                                |                   | Antwerp Member     |                 |                     | Genk Member      |                   |                      |                      |
|                                |                   |                    |                 |                     | Houthalen Member |                   |                      |                      |
|                                |                   | Kiel Member        |                 |                     | no deposits      |                   |                      |                      |
|                                |                   | Edegem Member      |                 |                     |                  |                   |                      |                      |

**Table 1.** The Miocene stratigraphic units in central and north Belgium, in the Roer Valley Graben and in the southern Netherlands. The term facies is used when a particular name has been given in descriptions without formally identifying this variety of sand as a separate lithostratigraphic unit. Note that Diest member in this table is proposed to indicate all sands of the Diest Formation except the Deurne and Dessel Members.

In the text Campine Diest member and Hageland Diest member are used to differentiate between the Diest member occurring in the two areas. 'No deposits' above the Deurne Member indicates that in the Antwerp area the Diest Formation is only represented by a thin Deurne Member, known by biostratigraphy to occur at the base of the Diest Formation which is much thicker developed in the Campine and Hageland areas. 'No deposits' between the Berchem and Bolderberg Formations represents the erosional removal of lower and middle Miocene deposits below the Hageland Diest Formation (see also Figs. 6 and 12).

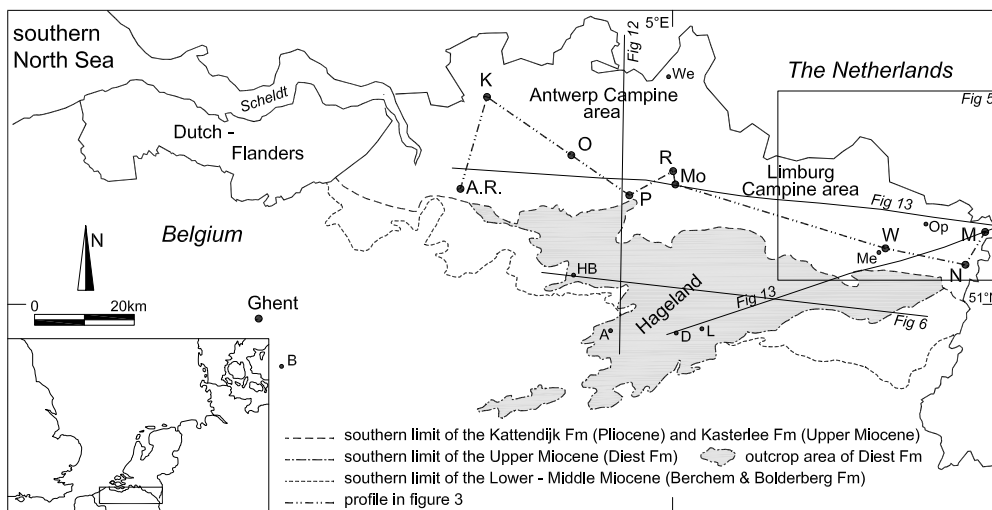


**Figure 1.** Location map. The profile along the line M-A.R. is shown in Fig. 3. The profile lines of Figs 6 and 13 are shown, the position of the profile sketches in Fig. 12 and the position of Fig. 5. Localities indicated are: M (Maaseik), N (Neeroeteren), W (Wijshagen), Me (Meeuwen), Op (Opitter), Mo (Mol), R (Retie), P (Poederlee), O (Oostmalle), K (Kalmthout-Essen), AR (Antwerpen-Rivierenhof), HB (Heist-op-den-Berg), A (Aarschot), D (Diest), L (Lummen), B (Balegem).

NE-SW, crosscutting the generally WNW-ESE striking, and slightly northward dipping, Paleogene and lower Miocene strata (Fig. 1). Expanding this NE-SW trend to the SW has made most investigators (Delvaux, 1884; Gullentops, 1957; Tavernier & de Heinzelin, 1962; 1:50 000 geological map Geraardsbergen) consider the formation on top of the residual hills in southwestern Flanders and northern France, which consists of glauconitic and limonitic sands like those in the Hageland hills, to be the Diest Formation. Nevertheless, no irrefutable evidence, neither paleontological nor mineralogical, has been found for such a correlation. Also, the depositional environment of the formation on top of the residual hills in southwestern Flanders and northern France was different (Houthuys, in review), so it will not be included in the discussion in the present paper.

Another geometrical feature of the Hageland Diest member is its uneven base, which results from the filling of deep incisions, where erosion had cut through the nearly 100 m thick Rupelian Boom Clay north of Aarschot and Diest (borehole Veerle 60E214). The incision axes have the same NE-orientation as the Hageland hills. The shapes of the hills were interpreted by Gullentops (1957) as relicts of offshore tidal sandbanks that emerged at the end of the deposition of the Diest member during the last marine transgression over the area.

The basal surface of the Diest Formation has recently been mapped over the entire area of occurrence (Matthijs et al., 2013)

(Fig. 2) and depicted on geological profiles (Matthijs et al., 2003). It appears from the morphology on this map and from the profiles that incisions below the Diest Formation, although less well expressed, also occur in the Campine area where the Diest Formation is known from many boreholes. The thickness of the Diest Formation in the Campine area reaches almost 100 m near the Dutch border.

Aside from the dominant Diest member, finer grained glauconitic and calcareous members occur in the Diest Formation. These are the laterally biostratigraphically equivalent Deurne Member in the west and the Dessel Member in the centre underlying the proper Diest member in the subsurface of the Campine area (Table 1; Fig. 3).

The precise stratigraphic position of the Diest Formation has been debated in the literature because of the general lack of calcareous fossils (see discussion in Vandenberghe et al., 1998). Louwye and coworkers (Louwye et al., 1999; Louwye & Laga, 1998, 2008; Louwye & De Schepper, 2010; Louwye et al., 2007) identified dinoflagellate cysts and proposed a more precise stratigraphic positioning of the Diest Sands in the Tortonian and the early Messinian (Figs 3 and 4). Remarkably, these organic-walled dinoflagellate cysts were recovered only from boreholes in the Campine area and never from the Hageland area.

The fine-grained Deurne and Dessel Members contain the same dinoflagellate cyst biozone DN8, some Dessel Member

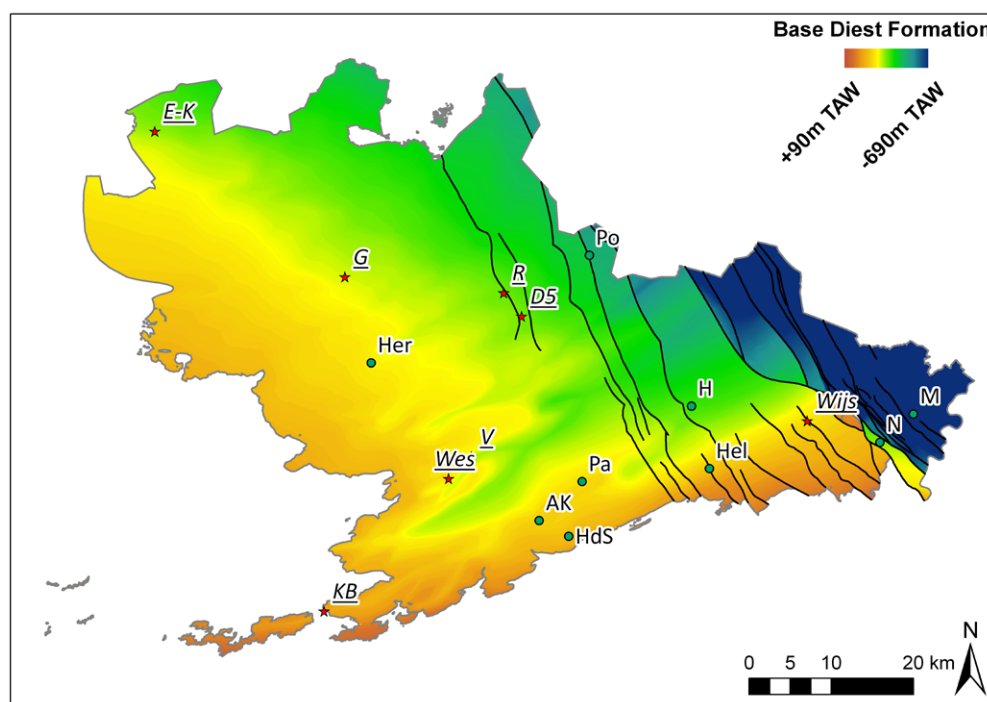
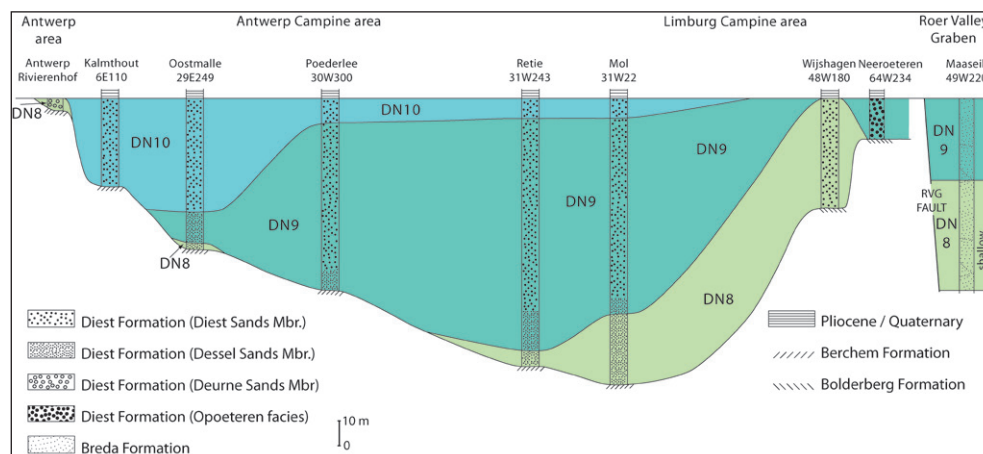


**Figure 2.** Borehole based map of the present day topography (TAW) of the base of the Diest Formation showing its marked morphology. The northern map limit is the Dutch-Belgian border and the southern limit is the southern occurrence of the Diest Formation (see Fig. 1). Locations indicated are the sampled boreholes Dessel-5 (DS), Essen-Kalmthout (E-K), Grobendonk (G), Hechtel (H), Helchteren (Hel), Herentals (Her), Herk-de-Stad (HdS), Maaseik (M), Neeroeteren (N), Paal (Pa), Postel (Po), Retie (R), Schaffen (AK), Veerle (V), Westerlo (Wes), Wijshagen (Wjs), and outcrop sample Kesselberg (KB). The samples analyzed for glauconite dating (Table 3) are indicated by a star.

**Figure 3.** Profile across the Diest Formation at the end of its deposition; the profile line from the Roer Valley graben in the east to the Antwerp area in the west is shown in Fig. 1. The members of the Diest Formation are shown together with the position of the dinoflagellate cysts biozones identified by Louwey (Louwey et al., 1999; Louwey and Laga, 2008; Vandenberghe et al., 2005). The interpretation of the Maaseik well lithostratigraphy is based on palaeontological content discussed in Vandenberghe et al. (2005); the shallow biofacies is not present west of the RVG boundary fault and the upper facies has a biofacies equivalent with Deurne and Dessel Sands biofacies west of the RVG boundary fault.



sands also contain biozone DN9, and were deposited during the earlier part of the upper Miocene (Louwey, 2002), consistent with previous foraminifera data (De Meuter & Laga, 1976; Hooyberghs & Moorkens, 2005). Further east in the Maaseik well, the top of the Breda Formation holds the same biozones as the Deurne and basal Dessel Members, biozone DN8 and in the top biozone DN9 (Vandenberghe et al., 2005); the early Tortonian dinoflagellate zone DN8 is also found in the Diest member of the Wijshagen well in the east (Louwey & Laga, 2008).

Within the Diest Formation in the north and east Campine area some particular lithological differences have been given informal names, such as the Opoeteren facies in the Neeroeteren well (Gulinck, 1964), the Gruitrode facies (Sels et al., 2001) and the glauconite-poor Poppel Sands in the top of the Diest Formation in the Weelde well (Laga & Notebaert, 1981).

A long standing issue in the upper Miocene paleogeography of the area is the stratigraphic position of the Diest Formation in the Hageland area, where all stratigraphically meaningful fossils are lacking. This adds to the uncertainty of the stratigraphic equivalence of the Hageland and the Campine Diest members.

### 3. The Hageland and Campine Diest Sands: the same or different units ?

The Hageland and Campine Diest members could be stratigraphically different sand bodies as indicated by the presence or absence of microfossils, the sedimentary petrology and mineralogy and the sediment transport directions. In addition major paleogeographic changes during Serravallian and Tortonian times have been documented in Western Europe.

The biozones identified in the Deurne Member outcrops and in the Dessel Member and Diest member of the Campine boreholes show that the Diest Formation spans dinoflagellate zones DN8, 9 and 10 (Fig. 3), stretching over almost the whole Tortonian and even part of the Messinian (Fig. 4). This represents a time interval of about 4 million years. Such a long period for a single sedimentary sequence is unusual for the regional Cenozoic sedimentary history, as discussed by Vandenberghe et al. (1998, 2004). The numerous unsuccessful attempts to recover calcareous or organic-walled microfossils from the Hageland Diest member could mean that either oxidation has caused the absence of dinoflagellates cysts so common in the Campine Diest member or that the Hageland Diest member simply never contained any microfossils.

Differences in heavy mineral content of the Hageland and Campine Diest members are evident in published data of Geets & De Breuck (1991), Gullentops (1963) and Gullentops & Huyghebaert (1999) and in a limited number of new analyses from localities specifically selected for the issue under discussion (Table 2). Compared to the Antwerp Campine area, the Hageland area heavy minerals are distinguished by a few percents of andalusite, high ubiquist content, low hornblende content and the near absence of garnet. Heavy minerals in the Dessel and

Deurne Members are similar to those in the Diest member from the Antwerp Campine. The Diest member heavy minerals from the eastern Limburg Campine (Meeuwen, Opitter, Wijshagen) resemble those of the Hageland Diest member rather than those of the Antwerp Campine, having very low hornblende and garnet, a few percents of andalusite and more tourmaline. These heavy mineral differences are not related to differences in grain size. Traditionally the garnet and hornblende are considered to have come from the northern marine realm and the andalusite from the southern continental area (Parfenoff et al., 1970). No shape differentiation can be made between the two Diest member areas; only a minor difference exists with the Houthalen Sands but Antwerp Sands are significantly less spherical and more angular than the others (for stratigraphy see Table 1). Glauconite contents, determined by magnetic separation, are similar in the Hageland and Campine Diest members, varying from 30% to 50%; only the lower 20 m of the Campine Diest member has lower glauconite contents, 20% to 28%.

In the Hageland area outcrops, large seismic-scale master clinoforms can rarely be observed, but smaller scale oblique strata are commonly observed; these represent migrating sand dunes, typically a few meters high, that probably make up the entire Hageland Diest member body. This oblique stratification shows that the sand prograded systematically to the northeast. The northeastward orientation of the progradation is the same as the orientation of the deeply incised valleys mapped at the base of the formation (Fig. 2). To explain this coincidence, Gullentops (1963, 1988) proposed that both erosion and fill were influenced by strong currents related to the existence during a sea-level high-stand of a

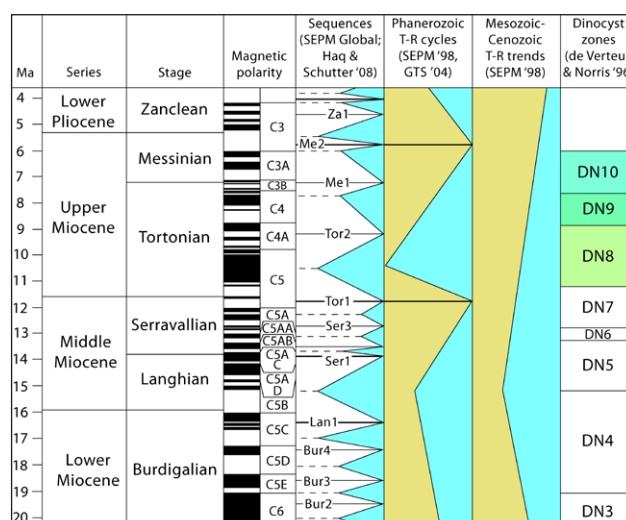


**Figure 4.** Dinoflagellate cyst biostratigraphy of the Miocene. The chronostratigraphy, magnetostratigraphy on the sequence stratigraphy are as shown in Hilgen et al. (2012); the Transgression (T)-Regression (R) cycles and trends are taken from Hardenbol et al. (1998).



| Member & Author           | Ubiquists |    |    | Parametamorphics |    |    |    | Ga | Ep | Ho |
|---------------------------|-----------|----|----|------------------|----|----|----|----|----|----|
|                           | To        | Zi | Ru | An               | Ky | St | Si |    |    |    |
| <b>Diest mbr Hageland</b> |           |    |    |                  |    |    |    |    |    |    |
| Author A                  | 17        | 36 | 16 | 3                | 6  | 5  | 1  | <2 | >8 | <2 |
| Author C                  | 16        | 38 |    |                  | 21 |    |    | 4  | 15 | 5  |
| <b>Diest mbr Limburg</b>  |           |    |    |                  |    |    |    |    |    |    |
| Author A                  | 15        | 40 | 16 | 2                | 5  | 5  | <1 | <5 | 4  | <5 |
| Author C                  | 10        | 55 | 15 |                  | 10 |    |    | 0  | 8  | 1  |
| <b>Diest mbr Antwerp</b>  |           |    |    |                  |    |    |    |    |    |    |
| Author A                  | 7         | 38 | 9  | <1               | 5  | 5  | <1 | 29 | 4  | 2  |
| Author B                  | 5         | 28 | 9  |                  | 10 |    |    | 33 | 8  | 7  |
| <b>Dessel Mbr</b>         |           |    |    |                  |    |    |    |    |    |    |
| Author A                  | 8         | 28 | 8  | <1               | 5  | 5  | <1 | 32 | 8  | 5  |
| <b>Deurne Mbr</b>         |           |    |    |                  |    |    |    |    |    |    |
| Author A                  | 11        | 25 | 10 | 1                | 6  | 4  | <1 | 30 | 8  | 5  |

**Table 2.** A summary of heavy mineral data of the Diest Formation. Author A: Geets & De Breuck, 1991 (24 samples Deurne Member, 123 samples Antwerp Campine Diest Formation, 46 samples Limburg Campine Diest Formation, 71 samples Hageland Diest Formation); author B: Gullentops & Huyghebaert, 1999 (11 samples); author C: Gullentops, 1963 (9 samples). The heavy minerals identified are Ubiquists (Zi: Zircon, To: Tourmaline, Ru: Rutile), Parametamorphics (An: Andalusite, Ky: kyanite, St: Staurolite, Si: Sillimanite), Ga: Garnet, Ep: Epidote, Ho: Hoornblende.

narrow, funnel-shaped marine connection of the North Sea to the Atlantic, like today's Dover Strait. In contrast, large scale internal clinoforms with a dip of about 5° in the Diest Formation have been imaged by traditional seismic reflection in the northeast Campine area (Demyttenaere, 1989) and by high-resolution seismics along the Campine canals (De Batist & Versteeg, 1999). Demyttenaere (1988) mapped the Campine subsurface, concluding that the large Hageland valley now filled with the Diest Formation sand was directly connected to the Roer Valley Graben (RVG) border in the northeast. Furthermore, he suggested that the history of erosion and fill was related to a fluctuating sea level in the Graben. An interplay must have existed between the global sea level, varying rates of graben subsidence, and uplift of surrounding land. However, most importantly, Demyttenaere (1989) noticed that in the northeast of the Campine area close to the Roer Valley Graben, a continuous pattern of large master clinoforms occurs with an apparent dip of the clinoforms of a few degrees to the southwest. The sediment progradation direction implied by this

observation was contrary to that expressed by the foreset dip of the Diest member cross-beds observed in the Hageland area, and Demyttenaere (1989) suggested a relationship with the Rhine delta sedimentation. Also, on the Campine canal seismic profiles east of the Dessel-Geel area (De Batist & Versteeg, 1999), similar large-scale low-angle clinoforms can be distinguished in the Diest member with apparent dip directions to the west-northwest and the north. In a recent interpretation of existing seismic lines in the Belgium-Netherlands border area, both NW and SSW sediment progradation directions were inferred between the bases of the Bolderberg (Table 1) and Kiezeloolith Formations (Deckers & den Dulk, pers.com.). When both progradation directions are evident in the same area, the sediments that prograded to the SSW are stratigraphically above those that prograded to the NW (Fig. 5). These progradations were part of a delta system that progressively filled the Roer Valley Graben during Miocene times. The Diest Formation was most likely part of this system, but the low resolution of the available seismic data and the lack of sufficient well log and biostratigraphic data hinder a clear outline of the Diest Formation bounding surfaces in the Roer Valley Graben. As Diest member sediment transport directions and provenance appear to be significantly different in the Campine and Hageland areas, the two sand masses may constitute different stratigraphic units.

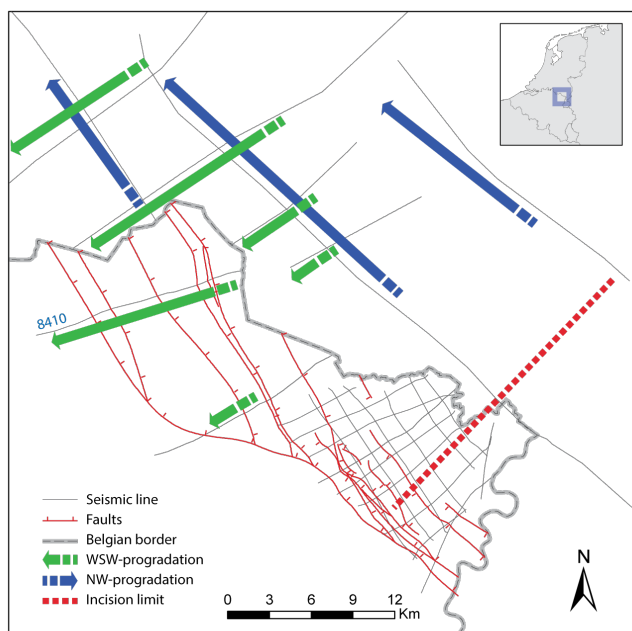


**Figure 5.** Orientation of sediment transport directions in the Diest Formation in the northeastern Campine and southern Netherlands subsurface inferred from the interpretation of oblique reflectors in seismic sections. Oblique reflectors dipping to WSW reported by Demyttenaere (1989) have been observed along line 8410. The sediments that prograded to the SSW are stratigraphically above those that prograded to the NW. The faults are bordering the Roer Valley Graben. SE of the incision limit no obvious erosional features were observed between the bases of the Bolderberg and Kiezeloolith Formations. Location of the figure is shown in Fig. 1.

The paleogeographic evolution of Western Europe during the Serravallian and Tortonian is compatible with major changes in sediment transport directions in lowland Belgium as described above. To the east the Campine area borders the Lower Rhine Graben. Sissingh (2003, 2006) has shown that between the early and middle Miocene the supply of clastics to the Lower Rhine Graben and the southern North Sea Basin changed. This change resulted when clastics arrived to the Lower Rhine Graben from the uplifting Ardennes and northeastern France and from the Upper Rhine Graben. There is little doubt that these changes are related to the end of the major peat deposition in the Lower Rhine area and the start of a new accumulation period of clastics forming the Inden Formation in Germany and the southern Netherlands at the beginning of the Tortonian. During the late Tortonian and later, coarse clastics prograded further towards the west and northwest over the marine glauconitic sands of the Breda Formation (Schäfer et al., 2004; Wong et al., 2007). It is also remarkable to note that massive prograding units occur above the so-called Mid-Miocene-Unconformity (MMU) further to the north in the North Sea (Kuhlmann, 2004) and also in the German North Sea (Vinken, 1988, fig. 266; Rasmussen and Dybkjaer, 2013); in the Lower Rhine Basin the MMU is estimated to occur during the Langhian (Utescher et al., 2007).

As several arguments discussed above suggest that the Diest Formation may not consist of a single stratigraphic unit and as age constraints are inadequate because of a lack of fossils, an attempt was made to obtain additional age information by radiometric dating of the abundant glauconite grains in the Diest Formation.

## 4. Glauconite ages

### 4.1. Selection of samples and sample preparation

Odin and Matter (1981) proposed the term glaucony as a facies name for authigenic pelleted material with no specific mineralogy, and either glauconitic mica or glauconitic smectite for end members of the specific mineral family. In this paper we have chosen to use the term glauconite rather than glauconitic mica. Glauconitic mica is considered to be an evolved to high-evolved mineral containing  $> 6\%$   $K_2O$ . Odin and Matter (1981), Odin (1982) and Keppens et al. (1984) suggested that glauconitic mica with less than  $6\%$   $K_2O$  are likely to give spurious K-Ar and Rb-Sr results.

Twenty-eight glaucony-rich samples were collected at the Belgian Geological Survey from a selection of boreholes suitable for an attempt to differentiate the Diest Formation occurring in the Campine area from that in the Hageland area. Furthermore, fresh outcrop samples were collected in the Hageland area and evaluated on suitability for dating. All samples were gently hand-crushed so that glaucony grain integrity was not destroyed, and screened into different size fractions identified by U.S. Standard Testing Screen Number. Glaucony from the selected size fractions was separated on the basis of its magnetic susceptibility with a Frantz Magnetic Separator. Separated size fractions were examined with a binocular microscope and by X-ray diffraction to determine those samples with a high potential for being authigenic with  $> 6\%$   $K_2O$  and capable of providing reliable dates. Using the criteria of Harris and Bottino (1974), Harris (1975), Odin (1975), Pasteels et al. (1976), and Keppens (1981), grains were selected and hand-picked by form (morphology), shape, degree of preservation, colour, and surface textures. Grains that were accordion-shaped, earthy, oxidized, broken, or contained foreign inclusions were removed by hand-picking. Impurities such as quartz, heavy minerals, and phosphate were also removed. Separation of the glaucony grains by magnetic concentration and hand-picking yielded 13 samples (12 boreholes, one outcrop) determined to have best opportunity to provide reliable dates. These samples were further studied by X-ray diffraction analysis (Table 3). Only one glaucony-rich outcrop sample at the base of the Diest Sands collected at the classical Kesselberg section near Leuven (Fig. 2) was selected for dating.

Samples selected by hand-picking generally had grains with a moderate to dark green color and little clay-size surface contaminants. Although it was hoped that only those glaucony grains that had well-preserved external morphologies would be selected for dating, grains in most samples exhibited some characteristics of reworking, including pitted and polished water-worn surfaces, dull lustre, and a lack of well-preserved external morphology (mammillated structure). However, the samples selected had the best potential of being evolved to well-evolved glaucony with a high- $K_2O$  content.

Each glaucony concentrate was washed in demineralized water, rinsed in reagent-grade acetone, and dried under a heat lamp. Each sample was also washed in reagent-grade 0.1 N HCl for 30-60 seconds to remove any possible carbonate contaminant. A second hand picking of impurities achieved a purity of  $>99\%$  glaucony grains. Based on binocular microscopic examination, the concentrates consisted of light-moderate green, to dark green to black, abraded mammillated grains; abraded grains were interpreted to be water-worn. Some grains were contaminated with minor tan to orange goethite in sutures, but such contamination was rare. One sample had two types of glaucony grains: dark green and tan green (H0924-60M in Table 3). The locations of the sampled and analysed outcrop and boreholes are indicated on Fig. 2.

All concentrates were examined by X-ray diffraction to determine the glaucony type following the techniques described by Odin (1982). This technique contributes significantly to the detection of low  $K_2O$  glauconitic samples that may contain non-glauconitic precursor minerals that could affect determined dates. Based on this analysis, the glaucony in all concentrates was determined to be evolved to highly evolved glauconitic mica (glauconite) with  $K_2O > 6\%$  of Odin and Matter (1981). A technique (FWHM) that employs the measured width of the basal X-ray diffraction peak (001) at half the maximum height of the peak from the baseline (Amorosi et al., 2007) was also used to examine the maturity of the glauconite concentrates. Amorosi et al. (2007) found that this technique resulted "... in a clearer discrimination of the different types of glauconite" and a better estimate of the  $K_2O$  content. Based on the FWHM technique, all samples dated contained greater than  $7\%$   $K_2O$ , confirmed later by chemical analyses (Table 3).

**Table 3.** Analytical results of the samples investigated for glauconite dating. The  $\pm$  error values represent  $2\sigma$ . The borehole numbers in the Sample column refer to the archives of the Belgian Geological Survey; the value between brackets is the topographic height of the outcrop or the borehole. In the Borehole depth column, (Diest) or (Dessel) indicates the lithostratigraphic member of the sample in the Diest Formation. <sup>1</sup>The test portion mass value is for the glauconite after drying overnight under vacuum. <sup>2</sup>Boldface values of mass lost on drying are for a set of test portions that were equilibrated with air over a saturated solution of magnesium nitrate ( $\sim 52\%$  relative humidity) before the original weighing. <sup>3</sup>The mass fraction of  $K_2O$  and the specific amount of radiogenic Ar are relative to the mass of dried glauconite. <sup>4</sup>Ar from the second portion of H0925-70M was, by mistake, not diluted with enriched <sup>38</sup>Ar. The amount of Ar from that portion was determinable, but with greater than usual error ( $\pm 5\%$ ), because the sensitivity of the mass spectrometer for Ar is nearly the same from one isotopic analysis to the next. Analytical procedure steps are further given in the text.

| Sample<br>(and Ar extraction temperature) | Borehole<br>Depth<br>(m) | Mass of<br>Test Portion <sup>1</sup><br>(mg) | Mass Lost<br>on Drying <sup>2</sup><br>(% by mass) | Potassium as<br>$K_2O$ <sup>3</sup><br>(% by mass) | Radiogenic Argon <sup>3</sup> |                          | K-Ar Date      |
|---|--------------------------|--|--|--|-------------------------------|--------------------------|----------------|
|   |                          |  |  |  | (% of <sup>40</sup> Ar)       | (nmol kg <sup>-1</sup> ) | (Ma)           |
| GL-O 1000°C                               |                          | 16.3   | <b>3.8</b>   | 8.25 $\pm$ 0.23                                    | 96                            | 1158 $\pm$ 33            | 95.1 $\pm$ 1.5 |
| <b>Kesselberg Outcrop (+60m)</b>          |                          |  |  |  |                               |                          |                |
| H0626 >60M 1000°C                         | NA (Diest)               | 29.7   | 3.1  | 7.46 $\pm$ 0.09                                    | 72                            | 157 $\pm$ 4              | 14.5 $\pm$ 0.4 |
| <b>Grobbendonk 29E 249 (+19.3m)</b>       |                          |  |  |  |                               |                          |                |
| H0924-60M 935°C                           | 33.0 (Diest)             | 41.9   | 3.6  | 7.42 $\pm$ 0.09                                    | 70                            | 188 $\pm$ 6              | 17.5 $\pm$ 0.6 |
| H0924-60M 1000°C                          |                          | 74.2   | <b>4.8</b>   | 7.41 $\pm$ 0.09                                    | 74                            | 190 $\pm$ 4              | 17.7 $\pm$ 0.4 |
| H0925-70M 935°C                           | 84.5 (Dessel)            | 39.2   | 3.7  | 7.77 $\pm$ 0.13                                    | 69                            | 191 $\pm$ 7              | 17.0 $\pm$ 0.7 |
| H0925-70M 935°C                           |                          | 69.4   | <b>4.4</b>   | 7.65 $\pm$ 0.10                                    | 68                            | 194 $\pm$ 11             | 17.6 $\pm$ 1.0 |
| H0925-70M reheated 1000°C <sup>4</sup>    |                          |  |  | 7.65 $\pm$ 0.10                                    | 32                            | 1 $\pm$ 1                | 0.1 $\pm$ 0.1  |
| <b>Kalmthout 6E 110 (+18m)</b>            |                          |  |  |  |                               |                          |                |
| H0930-60M 935°C                           | 84.0 (Diest)             | 50.5   | 2.9  | 7.98 $\pm$ 0.09                                    | 75                            | 198 $\pm$ 6              | 17.1 $\pm$ 0.5 |
| H0930-60M 1000°C                          |                          | 79.0   | <b>4.0</b>   | 8.09 $\pm$ 0.10                                    | 79                            | 189 $\pm$ 4              | 16.2 $\pm$ 0.4 |
| H0931-60M 935°C                           | 100.5 (Diest)            | 50.8   | 2.7  | 8.15 $\pm$ 0.09                                    | 75                            | 173 $\pm$ 6              | 14.7 $\pm$ 0.5 |
| H0931-60M 1000°C                          |                          | 61.4   | <b>3.5</b>   | 8.17 $\pm$ 0.11                                    | 80                            | 171 $\pm$ 5              | 14.5 $\pm$ 0.4 |
| <b>Retie 31W 243 (+20m)</b>               |                          |  |  |  |                               |                          |                |
| H0939-70M 935°C                           | 100.45-100.5 (Diest)     | 40.1   | 3.3  | 7.64 $\pm$ 0.09                                    | 70                            | 188 $\pm$ 7              | 17.0 $\pm$ 0.7 |
| H0939-70M 935°C                           |                          | 76.1   | <b>4.6</b>   | 7.57 $\pm$ 0.09                                    | 69                            | 187 $\pm$ 4              | 17.1 $\pm$ 0.4 |
| H0939-70M reheated 1000°C                 |                          |  |  | 7.57 $\pm$ 0.09                                    | 65                            | 2 $\pm$ 1                | 0.2 $\pm$ 0.1  |
| H0940-70M 935°C                           | 133.3 (Dessel)           | 45.9   | 2.9  | 7.99 $\pm$ 0.09                                    | 69                            | 159 $\pm$ 5              | 13.8 $\pm$ 0.5 |
| H0940-70M 1000°C                          |                          | 61.1   | <b>3.9</b>   | 7.99 $\pm$ 0.11                                    | 70                            | 158 $\pm$ 5              | 13.7 $\pm$ 0.4 |
| <b>Veerle 60E 215 (+20m)</b>              |                          |  |  |  |                               |                          |                |
| H0941-60M 1000°C                          | 53.2 (Diest)             | 53.6   | <b>4.4</b>   | 7.88 $\pm$ 0.11                                    | 72                            | 181 $\pm$ 5              | 15.9 $\pm$ 0.5 |
| H0942-60M 1000°C                          | 63.5 (Dessel)            | 65.4   | <b>4.4</b>   | 7.78 $\pm$ 0.10                                    | 72                            | 171 $\pm$ 5              | 15.2 $\pm$ 0.4 |
| H0943-60M 1000°C                          | 99.5 (Dessel)            | 70.8   | <b>4.7</b>   | 7.56 $\pm$ 0.10                                    | 69                            | 174 $\pm$ 5              | 15.9 $\pm$ 0.4 |
| <b>Wijshagen 48W 180 (+66m)</b>           |                          |  |  |  |                               |                          |                |
| H0945-60M 1000°C                          | 88.0 (Diest)             | 53.7   | <b>5.0</b>   | 7.40 $\pm$ 0.10                                    | 76                            | 163 $\pm$ 5              | 15.3 $\pm$ 0.5 |
| <b>Westerlo 60E 198 (+17m)</b>            |                          |  |  |  |                               |                          |                |
| H0948-60M 1000°C                          | 9.0-9.5 (Diest)          | 45.9   | <b>4.4</b>   | 7.88 $\pm$ 0.11                                    | 74                            | 169 $\pm$ 6              | 14.8 $\pm$ 0.5 |
| <b>Dessel-5 31W 370 (+25m)</b>            |                          |  |  |  |                               |                          |                |
| H0951-60M 1000°C                          | 139.1 (Dessel)           | 61.0   | <b>3.5</b>   | 8.35 $\pm$ 0.11                                    | 66                            | 137 $\pm$ 5              | 11.4 $\pm$ 0.4 |
| H0951-60M 1000°C                          |                          | 63.3   | 3.2  | 8.26 $\pm$ 0.11                                    | 66                            | 137 $\pm$ 5              | 11.5 $\pm$ 0.4 |

#### 4.2. K-Ar procedures

K-Ar measurements on the selected glauconite concentrates (Table 3) were done in the Department of Geosciences of Georgia State University, U.S.A., by procedures like those described by De Man et al. (2010). Measured ion beams were corrected (1) for mass discrimination, determined by isotopic analysis of Ar from air, (2) for small background signals due to hydrocarbons, calculated from measurement of the  $^{12}\text{C}_3^1\text{H}^+$  signal and an established cracking pattern for the hydrocarbons, and (3) for a small amount of Ar from air that leaked into the mass spectrometer at a known rate, assuming kinetic isotopic fractionation of the leaked Ar owing to different mean molecular speeds of the different isotopes. The Kesselberg outcrop sample was dated at Georgia Institute of Technology along with the glauconite samples dated by De Man et al. (2010). For this sample, there was no leak correction but there were small corrections for background signals due to HCl. Error values for mass fraction K, specific amount of radiogenic Ar, and K-Ar date were obtained by quadratic combination of estimated  $2\sigma$  relative errors for the independently measured quantities used in calculation of the derived quantities, as suggested by Dalrymple & Lanphere (1969, Eq. 7-1). Recommended values for decay constants and isotopic abundances reported by Steiger & Jäger (1977) were used in calculation of dates.

#### 4.3. K-Ar results

Two different temperatures were used for extraction of Ar, because the heater temperature for the first set of test portions was set lower (near  $935^\circ\text{C}$ ) than the intended temperature (near  $1000^\circ\text{C}$ ). To see if the lower temperature was sufficient, Ar was extracted from second test portions of two samples by first heating near  $935^\circ\text{C}$  and then again near  $1000^\circ\text{C}$ . The amount of radiogenic Ar extracted by the second heating near  $1000^\circ\text{C}$  was in each case less than 1% of the amount extracted in the first heating. Ar was extracted at near  $1000^\circ\text{C}$  from second test portions of the four other samples that had been included in the first set, and there is in no case a significant difference in specific amount of radiogenic Ar extracted at the different temperatures.

Accuracy of the K and Ar measurement procedures was confirmed by using them to obtain a date of  $95.1 \pm 1.5$  Ma for the interlaboratory reference glauconite sample GL-O (Odin, 1982). Comparison of analytical results from duplicate portions of seven of the glauconite samples indicates that the assigned  $2\sigma$  error values are appropriate. The Ar from the second portion of HO925-70M was, by mistake, not diluted with enriched  $^{38}\text{Ar}$ . The amount of Ar from that portion was determinable, but with greater than usual error ( $\pm 5\%$ ), because the sensitivity of the mass spectrometer for Ar is nearly the same from one isotopic analysis to the next. No measurable amount of either K or radiogenic Ar was found when an empty capsule was used for a procedural blank.

Glauconite concentrates from 13 samples (12 in bore holes, one outcrop) were dated. K-Ar analytical data, obtained dates including individual results from systematic repeated analyses in parentheses below, are given in Table 3. Below, results are given by age.

**Burdigalian** – Four glauconite concentrates provided Burdigalian ages and included two samples from Grobbendonk borehole, one sample from Kalmthout borehole, and one sample from Retie borehole. Widely separated glauconites from depths of 33 m and 84.5 m in Grobbendonk provided analytically identical results of  $17.5 \pm 0.6$  Ma ( $17.7 \pm 0.4$  Ma) and  $17.0 \pm 0.7$  Ma ( $17.6 \pm 1.0$  Ma), respectively. A glauconite concentrate from Kalmthout borehole at 84.0 m provided a date of  $17.1 \pm 0.5$  Ma ( $16.2 \pm 0.4$  Ma), and a concentrate from Retie borehole at 100.45–100.5 m provided a date of  $17.0 \pm 0.7$  Ma ( $17.1 \pm 0.4$  Ma).

**Langhian** – Six borehole and one outcrop glauconite concentrates provided Langhian ages. Kalmthout at 100.5m yielded a date of  $14.7 \pm 0.5$  Ma ( $14.5 \pm 0.4$  Ma), Veerle at 53.2, 63.5 m, and 99.5 m dates of  $15.9 \pm 0.5$  Ma,  $15.2 \pm 0.4$  Ma, and  $15.9 \pm 0.4$  Ma, respectively, Wijshagen at 88.0 m a date of  $15.3 \pm 0.5$  Ma, and

Westerlo at 9.0–9.5 m a date of  $14.8 \pm 0.5$  Ma. Glauconite at the Kesselberg outcrop yielded a date of  $14.5 \pm 0.4$  Ma.

**Serravallian/Langhian** – One glauconite concentrate, 133.3 m in the Retie borehole, yielded a Serravallian age of  $13.8 \pm 0.5$  Ma ( $13.7 \pm 0.4$  Ma) or Langhian age considering the error.

**Tortonian** – One glauconite concentrate, 139.1 m in the Dessel-5 Borehole, yielded a Tortonian glauconite date of  $11.4 \pm 0.4$  Ma ( $11.5 \pm 0.4$  Ma).

#### 4.4. Discussion of K-Ar results

The most obvious conclusion from comparing the dinoflagellate cyst based ages in the Campine Diest Formation and the glauconite dates from the Diest Formation reported in Table 3 is that the biostratigraphically determined Tortonian age (7.25–11.63 Ma, Hilgen et al., 2012) is very different from the glauconite dates; dates from the Dessel-5 borehole are an exception. As the numerous biostratigraphical ages are consistent, they reliably point to a Tortonian age for the Diest Formation and require an explanation for glauconite dates that correspond to earlier ages, Langhian (15.97–13.82 Ma) and Burdigalian (20.44–15.97 Ma).

##### 4.4.1. The base of the Dessel Member (139–139.5 m) in the Dessel-5 borehole.

Closely consistent duplicate glauconite dates of a sample from the base of the Dessel Member (139–139.5 m) in the Dessel-5 borehole of  $11.4$  and  $11.5 \pm 0.4$  Ma are of Tortonian age, or the very latest Serravallian, and may represent the age of the deposit itself. In the neighboring Retie and Mol wells, the lower sands contain dinoflagellate cyst biozone DN8 (Fig. 3), which corresponds to the base of the Tortonian. The similar lithology of these basal sands and those in Dessel-5 suggest they are correlative and support the glauconite dates as representing the age of the deposit. The geophysical well logs (Labat et al., 2011) show at the sampling level rising radioactivity and density values and decreasing resistivity values, corresponding to a higher glauconite content than is usually observed in the Dessel Member (37% vs. 25% respectively). One meter below the sampled level a coarser level represents the base of the Diest Formation. These glauconite dates, therefore, are interpreted to represent the formation time of the glauconite right before it was concentrated and swept over the transgressive surface to form a green sand at the base of the Diest Formation.

##### 4.4.2. Hageland samples Westerlo, Veerle and Kesselberg.

The Hageland samples of the Kesselberg outcrop and the boreholes Veerle and Westerlo show a consistent group of Langhian glauconite dates from  $14.5 \pm 0.4$  Ma to  $15.9 \pm 0.5$  Ma. The Westerlo sample is Diest Sands from a shallow borehole at 9–9.5 m depth. The Kesselberg sample is from a greensand (66% glauconite) right above the eroding base of the Diest Sands. The Veerle borehole is from a location where the pre-existing terrain had been deeply eroded to the base of the Oligocene (Fig. 6) (Gulinck, 1973). The Veerle borehole samples (Table 3) are from the Diest member (53.2 m), and from the top (63.5 m) and the basal part (99.5 m) of the Dessel Member (Gulinck, 1973). In the Dessel Member section of this borehole samples at 96.8 m and 103.5 m contain dinoflagellate cysts of the lower Tortonian DN8 zone (Louwyte, unpubl.).

##### 4.4.3. West and Central Campine samples Grobbendonk, Kalmthout and Retie.

The glauconite dates of the discussed Hageland samples Veerle, Westerlo and Kesselberg, between  $14.5 \pm 0.4$  Ma to  $15.9 \pm 0.5$  Ma, Langhian, are different from the dates found in the West Campine samples Grobbendonk (base and top) and Kalmthout (top), and in the Central Campine Retie (top), which are from  $16.2 \pm 0.4$  Ma to  $17.7 \pm 0.4$  Ma (Table 3), all being Burdigalian. The Hageland dates are however close to those of samples from the base of the Diest Fm in the Kalmthout (100.5m),  $14.5 \pm 0.4$  and  $14.7 \pm 0.5$  Ma, and Retie (133.3m),  $13.7 \pm 0.4$  and  $13.8 \pm 0.5$  Ma, boreholes and from the Diest member in the Wijshagen borehole in the eastern Campine,  $15.3 \pm 0.5$  Ma.



#### 4.4.4. The Wijshagen sample from the eastern Campine area.

Wijshagen is located in the eastern Campine area (Figs. 1 & 2) and the sands of the Diest member in that well have a glauconite date of  $15.3 \pm 0.5$  Ma, consistent with the Hageland samples. The sample was taken from near the base of the Diest member, which overlies in that area the Houthalen Sands (Table 1) of latest early to middle Miocene age (Louwye & Laga, 2008). The Wijshagen well is at the most east-northeastward extension of the Diest Formation located there at moderate depth (see Fig. 2). Erosive valleys at the base of the Diest Formation occur also in the eastern Campine area and are aligned with the orientation of the Hageland hills (Figs. 2 & 5) (Matthijs et al., 2003). As discussed earlier, the heavy mineral association of the eastern Campine Diest member, from Lummen to Opitter, resembles the heavy mineral association of the Hageland Diest member rather than the Antwerp and Central Campine (Mol, Retie) Diest member association. Therefore, the glauconite date of the Wijshagen Diest Sands apparently confirms that the Diest member in the eastern Campine area can be considered as an extension of the Hageland Diest member towards the RVG as discussed above (see also Fig. 12). Also, as stated above, the Hageland dates and the basal Retie and Kalmthout dates overlap when the error is considered (Table 3).

In conclusion, except the basal Dessel-5 sample which represents a very early Tortonian age of the Dessel Member, the glauconite dates obtained can be subdivided in two groups. The first one groups the Hageland, the basal Retie and Kalmthout, and the Wijshagen samples and shows dates that point to a Langhian age. The second group includes the Grobbendonk, upper Retie and upper Kalmthout samples of the western and central Campine that point to a Burdigalian age. Regarding the Campine samples in both groups, for which biostratigraphic evidence clearly indicates Tortonian ages, the only possible conclusion is that the glauconite grains were *in situ* altered or reworked. The same applies also to the Wijshagen sample as the Tortonian biozone DN8 was reported for the entire Diest Sands section in the borehole (Louwye & Laga, 2008) (Fig. 3). Because Wijshagen glauconites have similar dates as the Hageland samples but the latter have no biostratigraphical control, logically these Hageland glauconites should also have been altered *in situ* or reworked. It is indeed logical that the Hageland Diest member was not deposited during the Langhian but later during the Tortonian because the formations eroded to form the Hageland valleys, namely Antwerp Sands, Zonderschot Sands and Houthalen Sands (Table 1), all contain dinoflagellate cysts of Langhian age, the Antwerp and Houthalen Sands even extending over the full Langhian time range (Louwye & Laga, 2008). Therefore it is highly improbable that the Hageland Diest member could also have been deposited during the Langhian.

As *in situ* altering would likely have led to glauconites apparently younger than their host sediments, which is not the case in the present study, only reworking remains a plausible explanation for the glauconite date results. This reworking must have been massive, given the glauconite content of the Diest Formation in the Campine and the Hageland areas: between 16% and 67% with an average of 40% in the Campine area (60 samples) and between 11% and 58% with an average of 39% in the Hageland area (15 samples). Reworked pre-upper Miocene

dinoflagellate cysts were observed in every studied sample of the Diest Formation at every location. For instance, in the cored Kalmthout well the reworking varies between 13.9% and 0.4%, with a mean value of 6.2% (Louwye & Laga 1998). These figures do not include the long-ranging species of the genus *Spiniferites*. Furthermore, mechanical degradation during transport resulted in the poor preservation of the reworked cysts.

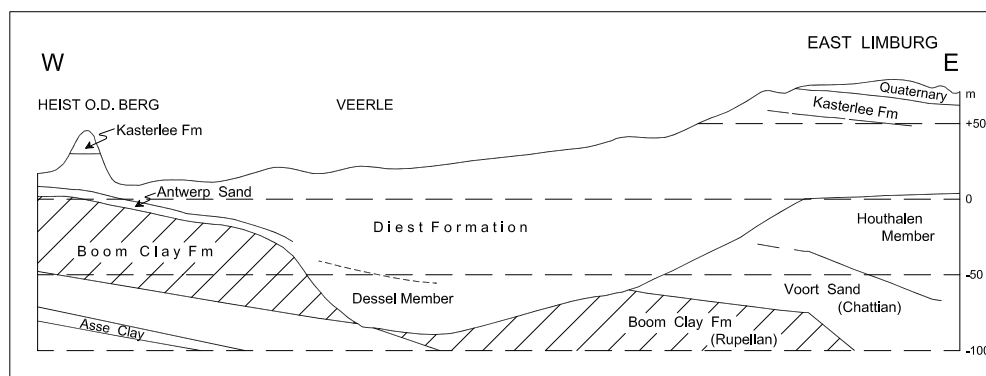
### 5. Stratigraphic age of sediments eroded and reworked in the Diest Formation.

In this section potential sources of the reworked glauconitic sediments and their stratigraphic ages are investigated to determine if they can explain the glauconite dates in the Diest Formation. As the reworked Diest Formation glauconite dates cluster into two groups, mainly Langhian in the Hageland area and eastern Campine area and in the basal parts of the Retie and Kalmthout boreholes, and Burdigalian in the western and central Campine Basin, an explanation is required for their differentiation. In addition, sediments with older glauconites occur on top of sediments with younger glauconites (see Kalmthout and Retie boreholes in Table 3).

On regional geological profiles (Matthijs et al., 2003 and e.g. Fig. 6) it can be observed that the complex Hageland channel eroded in its western part about 10 m of the Berchem Formation and in the east 40 to 50 m of Houthalen Sands. The Houthalen Sands extend as far as Leuven, Brussels and possibly originally as far west as Ghent, as shown by the occurrence of the typical egg-shaped dark bluish flints of their basal gravel, *in situ* or reworked in the Quaternary (observation in the Balem sand pit, location see Fig. 1). From the geological profiles (Matthijs et al., 2003) it is obvious that the Berchem Formation was strongly eroded not only where the valleys underlie the Hageland area but also under the Diest Sands of the central and western Campine, where up to 50 m of Antwerp Sands of the Berchem Formation are still preserved in some areas. The Edegem and Kiel Sands, older lower members of the Berchem Formation (Table 1) are not relevant for the present discussion as they occur only in a limited area to the southwest of the Diest Formation (maps of Laga, 1973, 1982). Based on dinoflagellate cyst stratigraphy (Fig. 4) both the Houthalen Sands and the Antwerp Sands are *in-situ* mainly of Langhian age (Louwye & Laga, 2008).

The Antwerp and Houthalen Sands consist of several subunits that are not easily recognizable. The Zonderschot Sands for example (Louwye, 2000) can be considered as a subunit of the Antwerp Sands (Table 1). This variability could explain the quite varying biozonations reported for the Antwerp and Houthalen sands, within the Burdigalian and Langhian and even sometimes the Aquitanian and Serravallian (reviews by Vandenberghe et al., 1998; Louwye & Laga, 2008). For example even the more recent dinoflagellate cyst analyses report biozones DN2 (uppermost Aquitanian to Burdigalian) in the Antwerp Sands of the Kalmthout well (Louwye et al., 1999), DN3 (Burdigalian) in the Antwerp Sands of the central Campine (Louwye et al., 1999), DN4 (Burdigalian to Langhian) in the Antwerp and Zonderschot Sands (Louwye & Laga, 2005), DN5 (Langhian to Serravallian) in the Antwerp Sands (Louwye et al., 1999; Louwye & Laga, 2005), and possibly DN6 or DN7 (upper Serravallian) in the Antwerp Sands in the Borgerhout Rivierenhof outcrop (Louwye

**Figure 6.** Profile from Heist-op-den-Berg (location HB and profile in Fig. 1), across the Veerle borehole to eastern Limburg (simplified after Gulinck, 1973) showing the erosion of the Diest Formation valley (Veerle borehole) eroding Houthalen Sands in the east and Antwerp Sands in the west.



et al., 2000). DN6 and DN7 biozones have also been found in green glauconitic sands in the Maaseik well (Vandenberghé et al., 2005). In the Houthalen Sands of the Wijshagen borehole biozones DN4 and DN5 restrict the age of the sands to the Langhian. Therefore dinoflagellate cyst biostratigraphy could suggest that the main mass of reworked glauconite in the Diest Formation group with Langhian dates is mainly derived from the Houthalen Sands occurring in the east, southeast and south and that the reworked glauconites in the Diest Formation group with Burdigalian ages are mainly derived from the Antwerp Sands occurring in the north and northwest.

For the original Houthalen Sands, unfortunately, no glauconite dates are available to confirm this hypothesis. However, glauconite dates of the older Berchem Formation underlying the Campine area were given by Odin et al. (1974) and confirmed in a methodological study by Pasteels et al. (1976). The Antwerp Sands Member of the Berchem Formation has glauconite dates between 16 and 19 Ma while the deeper members Edegem and Kiel, not relevant for our study, have glauconite dates exceeding 22 Ma; a glauconite date of  $15.1 \pm 1.0$  Ma was reported by Odin et al. (1974) for the Zonderschot Sands occurring at the border of the Antwerp Campine and the Hageland area (Heist-op-den-Berg, see Fig. 1). Keppens & Pasteels (1982) noted that glauconite ages from a Campine Diest Sands sample, from a borehole at Mol, and from a sample of the Zonderschot Sands were comparable and suggested therefore a reworking of the Diest Sands glauconite from underlying sediments.

Reworking is also expressed in the sediment properties. An analysis in both the Antwerp Sands and the sands of the Diest member of the Essen-Kalmthout borehole shows that glauconite grains are comparable in size but the modal quartz-grain size in the former is much smaller than in the latter (Fig. 7). Therefore, based on size, glauconites and some of the finest quartz in the Diest member could have been derived from the Antwerp Sands but the coarser quartz in the Diest member must have been derived to a large extent from another source. Note also in Fig. 7 that in the Antwerp Sands glauconite size is larger than quartz size and in the Diest member glauconite size is smaller than quartz size, suggesting authigenic glauconite in Antwerp Sands, as was also concluded from the dating results by Odin et al. (1974), but transported glauconite in the Diest Sands; this interpretation is based on the density difference between glauconite and quartz. In addition the glauconite dates of the Diest member examined in this study display evidence of reworking based on surface abrasion and polish as previously mentioned. Estimating volumes of reworked Antwerp Sands in the Diest Formation is difficult because the spread in glauconite content in both units and the unknown degree of quartz-glaucanite separation during reworking. However with e.g. 35 to 40% glauconite in the Diest Formation, all derived from Antwerp Sands, and 60% in the Antwerp Sands (up to 70% in the Antwerp area (Bastin, 1966) and on average 48% in the Campine area in this study), and all quartz in the Diest Formation derived from another source, more than half of the present Diest Formation is derived from reworked Antwerp Sands. The large range of biostratigraphic ages reported

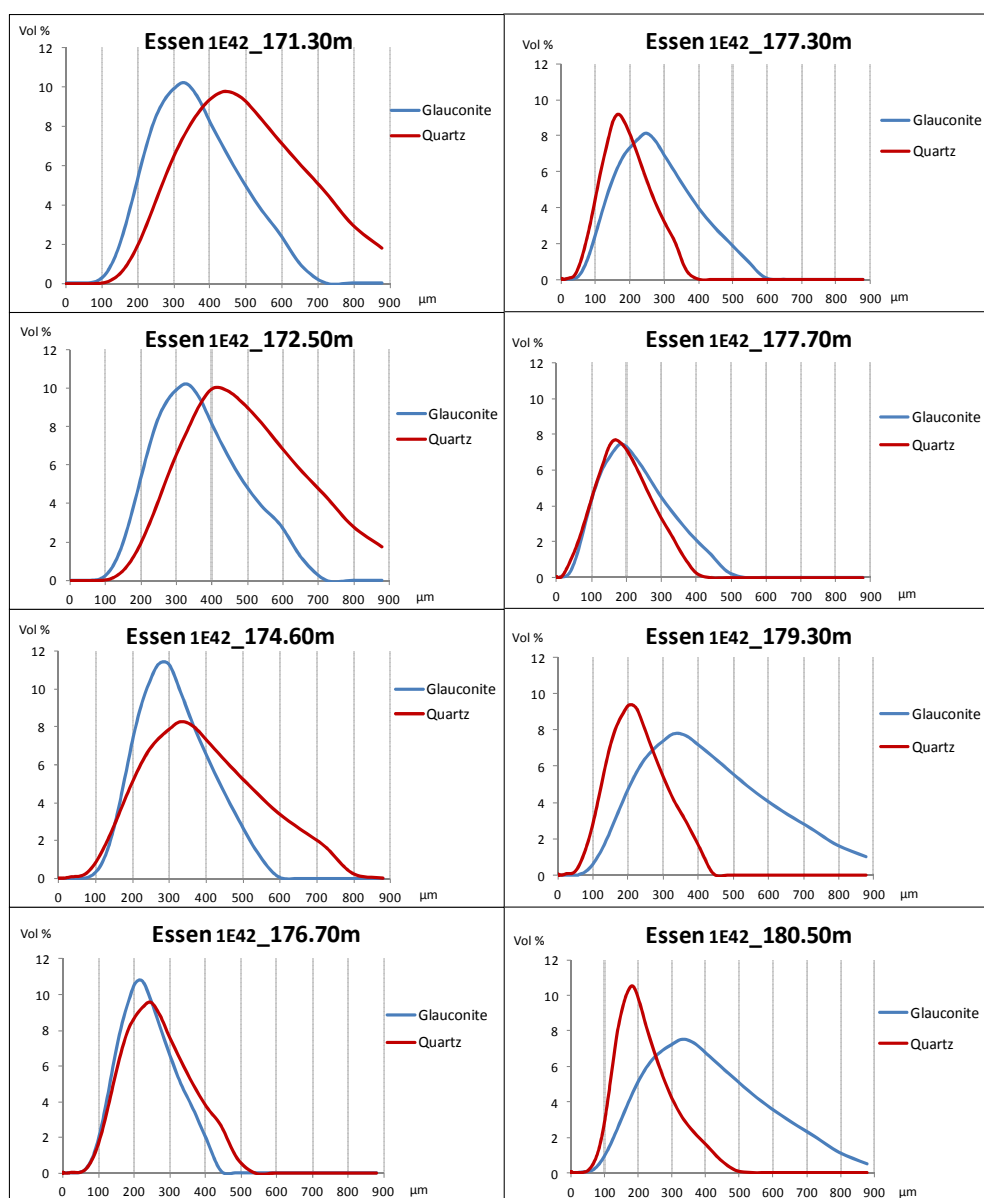
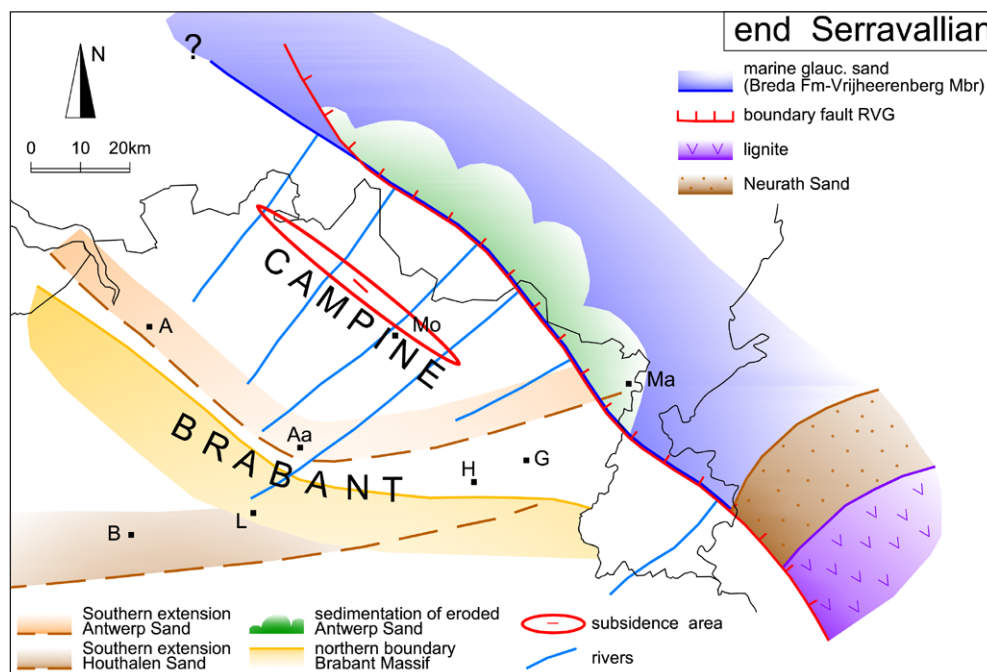


**Figure 7.** Size analysis of glauconite and quartz grains at different depths in the borehole Essen (location Kalmthout-Essen in Figs 1 & 2). In the left column the grains belong to the Diest member and in the right column to the Antwerp Member. Note that in the Antwerp Sands glauconite grains have a larger modal size than the quartz. In the Diest member glauconites have comparable sizes as in the Antwerp Sands but the quartz modal size is larger than the glauconite modal size. The quartz grains in the Diest member are significantly larger than in the Antwerp Sands.



**Figure 8.** Sketch of the end Serravallian paleogeography. The sediment distribution in the graben is after Schäfer et al. (2004) and Wong et al. (2007) and the lignite extension after (Gliese & Hager, 1978). A system of parallel rivers is draining a sloping Campine land surface from the south to the sea in the north which is contained in the Roer Valley Graben (RVG). Antwerp Sands eroded by the rivers are deposited in the subsiding RVG. Ma (Maaseik), Mo (Mol), A (Antwerp), Aa (Aarschot), B (Brussels), L (Leuven), H (Hasselt), G (Genk).



in the Antwerp Sands as discussed above can also be interpreted as an indication that much larger volumes of Antwerp Sands may have existed in the past than are preserved today. It is also very well possible that Antwerp Sands were reworked from the area to the west-northwest of Antwerp in the Netherlands, where these sands are now completely lacking and where in some localities Deurne Sands directly overly Oligocene clays (van Rummelen, 1977). Reworking of Houthalen Sands with 7% to 27%, on average 19%, glauconite content (5 samples) would require concentration of the glauconite in the Diest Formation.

It should also be remembered that the presence of some Tortonian glauconites, like those at the base of the Dessel-5 borehole, mixed with the reworked glauconites could cause a spread in the glauconite dates. The lack of an obvious effect of Oligocene or Eocene glauconites on the dates of the reworked glauconites of the Hageland Diest member can be understood because the sediment volume of such stratigraphic intervals eroded by the Hageland valley are either small or do not contain abundant glauconite (see Fig. 6).

In conclusion, the new glauconite data combined with existing biostratigraphic data and the general geological history of the area demonstrate that the Diest Formation must consist to a large extent of reworked older sands. There is evidence for authigenesis of glauconite at the very beginning of the Tortonian and such glauconite might have influenced the younger glauconite ages obtained at the base of the Diest Formation in the Retie and Kalmthout boreholes in the Antwerp Campine (see Table 3). The Burdigalian dates of reworked glauconites in the Antwerp Campine Diest Formation, upper Retie and upper Kalmthout boreholes, are similar to the previously determined radiometric dates of authigenic glauconite in the Antwerp Sands. The Langhian dates of reworked glauconite in the Hageland area and its border area in the northeast at Wijshagen correspond to the biostratigraphic age of the Houthalen Sands and to a radiometric date previously obtained from an upper Antwerp Sands facies (Zonderschot facies, Table 1) at the northwestern border of the Hageland area (Heist-op-den-Berg).

## 6. Implications for the paleogeographic evolution

In this section a paleogeographic evolution from late Serravallian to the end Tortonian is sketched, integrating the earlier discussed data on the Diest Formation in the Hageland and the Campine areas and the massive reworking implied by the results of the glauconite dating. The proposed sketches are by no means final reconstructions, because a major difficulty in reconstructing the paleogeography of the Diest Formation is the lack of precise sedimentological data. The sediments at the top of the Flemish

hills in northern France and south Flanders and the Lenham beds near Maidstone in East Anglia are traditionally attributed to the Diest Formation but are less well preserved and not well documented, so they are left out of the paleogeographic sketches developed below (see also Houthuys, in review).

### 6.1. Late Serravallian (ca 12 Ma) (Fig. 8)

Subsidence of the Campine relative to the Brabant area south of it occurred during the Burdigalian and Langhian as shown by the present distribution of the Antwerp Sands Member of the Berchem Formation (Fig. 8). The area south of the Campine overlies the vertically mobile Brabant-Ardenne Massif (Fig. 8). Differential vertical tectonic movement between a subsiding Campine and a rising southwestern area in the Oligocene, when the Lower Rhine Graben started a significant subsidence, has already been documented in the Antwerp area (De Man et al., 2010; Vandenberghe & Mertens, 2013). The Serravallian was a time of uplift in northern France and southwest Belgium (Van Vliet-Lanoë et al., 2002, 2010). Sedimentation was probably restricted to the fault-scarp-bounded Roer Valley Graben. Seawards, peat in the graben was replaced by the estuarine to shore-face facies of the Neurath Sands, and, further in the Netherlands, by the Vrijheerenberg Member of the Breda Formation (Wong et al. 2007) (Table 1), an open marine argillaceous greensand (Fig. 8).

The Campine area was a land surface and a consequent river system pattern caused incisions that can be recognized in the map of the basal surface of the Diest Formation (Fig. 2). A series of parallel rivers drained northeastward in the direction of the Roer Valley Graben hosting a fault-contained sea. A consequent pattern typically develops on an even and mildly sloping land surface. The more pronounced troughs in the Diest Formation basal surface occur in the south (Fig. 2), close to the present southern boundary of the Diest Formation. This is also approximately the southern limit of the occurrence of the Antwerp Sands (Berchem Formation) on which the river system had developed. As discussed above, the wide range of biozones from Burdigalian to Serravallian in the Antwerp Sands suggests that originally a thick deposit of Antwerp Sands was present in the Campine probably extending to the northwest into the Netherlands. It can be supposed that the main mass of these Antwerp Sands was eroded by the rivers and deposited as a line of submarine fans over the fault bounded coast line and further seawards to the northwest, to be redistributed by the currents and form a coastal sand body (Fig. 8). In the Maaseik well, just across the boundary fault inside the graben (Fig. 8), the green glauconitic sand with the dinoflagellate cyst biozones DN6 and DN7 at the base of the core (Vandenberghe et al., 2005) is interpreted as redeposited Antwerp Sands.

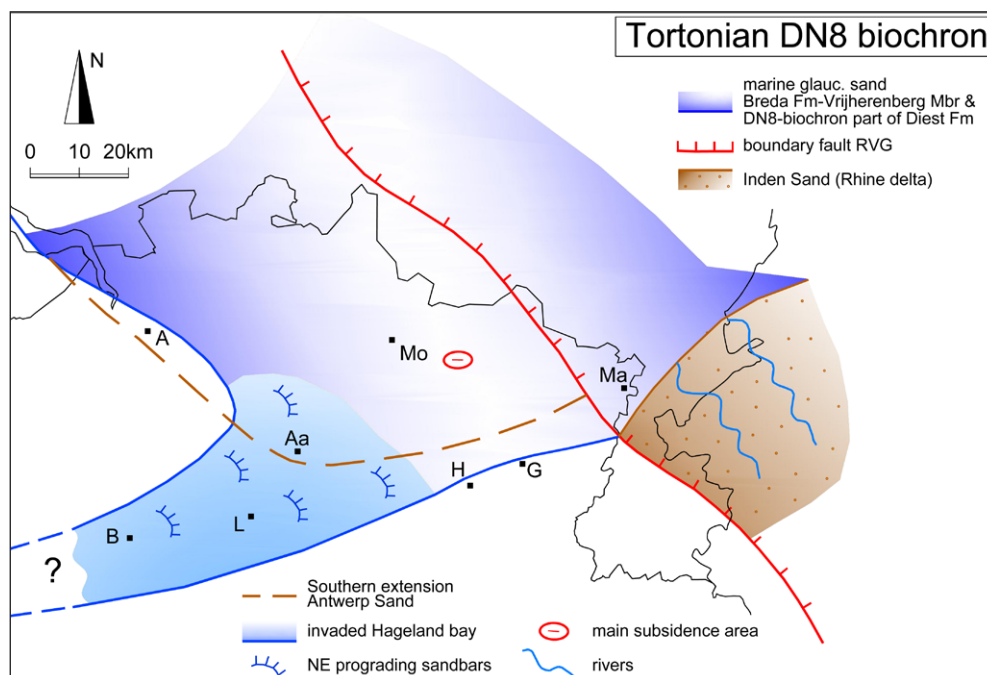


**Figure 9.** Sketch of the lower Tortonian DN8 biochron paleogeography. A transgression covered the whole Campine area forming the Deurne and Dessel Members; the Hageland valleys were transformed in a broad bay. During the sea-level high-stand-systems-tract the Hageland sand bodies were deposited in the bay, prograding in the north over earlier deposited transgressive deposits and continuing along the coast into northeast Limburg. Ma (Maaseik), Mo (Mol), A (Antwerp), Aa (Aarschot), B (Brussels), L (Leuven), H (Hasselt), G (Genk).

The erosion occurred in the interval between the youngest deposited Antwerp Sands (DN6 or DN7, Rivierenhof outcrop near Antwerp, Louwye et al., 2000) and the oldest Diest Formation sediments (DN8).

## 6.2. Early Tortonian DN8 biochron (ca 11-9 Ma) (Fig. 9)

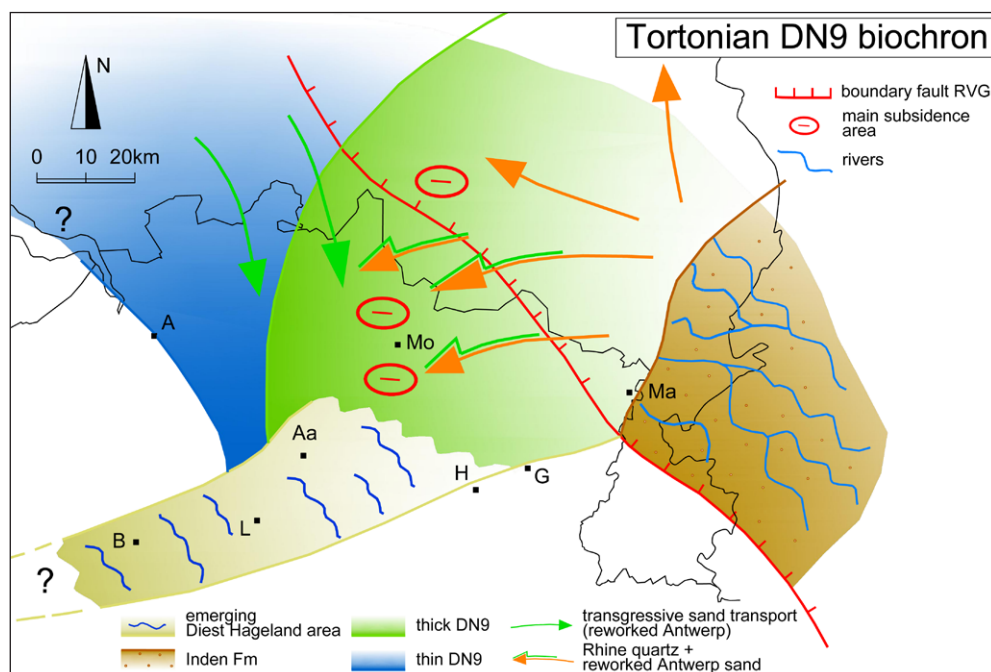
A renewed shallow marine incursion from the north into the subsiding Campine basin is represented by the Deurne Sands and that part of the Dessel Sands containing the dinoflagellate cyst biozone DN8 (Fig. 3). Glauconite may have formed at the beginning of this transgression as indicated by the Dessel-5 glauconite date discussed earlier. The marine influence, maybe a broad bay, can be traced as far south as Antwerp, Veerle and Maaseik and is drawn on Fig. 9 based on the present occurrence of Deurne and Dessel Sands in boreholes, in the Belgian Geological Survey archives and on the geological map of the Dutch Flanders (Zeeuws-Vlaanderen) (van Rummelen, 1977). It may very well have been situated further south, at the present southern boundary of the Hageland Diest Sands, where later submarine erosion removed all early transgressive deposits. During this early Tortonian biochron DN8, the central to eastern part of the Campine (Mol, Wijshagen and Maaseik wells) subsided the most (Fig. 3) and the areas of the Veerle well and the later Hageland were adjacent to this subsidence area. In the northeast the quartz-rich X-unit above the DN8 containing glauconite sand in the Maaseik well described by Vandenberghe et al. (2005), may represent the Inden Formation prograding over the glauconitic Breda Formation (Dusar, pers.com.). The Inden Formation is a meandering river facies that formed in the Rhine delta plain (Schäfer et al., 2004, fig. 7).

The DN8 biochron Dessel-Deurne transgression was not energetic because the inherited valley morphology at its base is preserved as shown in Fig. 2. This suggests sea-level rise in a sheltered bay resulting from an initial sea incursion in the pre-DN8 river valleys, possibly helped by subsidence. As sea level continued to rise, the water invaded those valleys in the east where the Campine basin was subsiding most during biochron DN8. This resulted in a broad embayment in the present Campine and Hageland areas (Fig. 2). Gullentops (1957), followed by Houbolt (1982), interpreted the sedimentary environment of the Hageland Diest Sands as a near-coast continental shelf showing a system of tidal offshore sandbanks, built of medium to coarse glauconitic sand, that after the final regression of the sea are preserved in the present-day Hageland hill topography. This interpretation is problematic in that it does not account for the fact that the sands of the Diest member are preserved as a sand deposit in a filled basin whose long axis is inland of and perpendicular to the contemporary coastline, nor for the deep channels at their

base and the outstandingly unidirectional nature of the currents that deposited the sand. Meters-thick cross-beds with foreset laminae dipping exclusively to the NE dominate in the Hageland Diest member. They suggest strong currents that flowed to the NE, i.e. towards the sea in the Roer Valley Graben. Therefore Demyttenaere (1988) interpreted the Hageland Diest Formation as having filled an incised valley system. However, in contrast to the common variety of sedimentary lithofacies in drowned incised valleys (Zaitlin et al., 1994; Dalrymple & Choi, 2007), the Hageland Diest member consists of a narrow range of marine tidal-current sand facies. Also, some depressions in the basal surface appear to be closed at their downstream end (map in Houbolt (1982) based on data collected by Van Calster in the 1960s), which is incompatible with a drowned incised valley system. Houthuys (subm., fig. 7) proposed an alternative depositional environment based on a reinterpretation of the sedimentary facies and their geometry, which show a high similarity to the Eocene Brussels Sands (Houthuys, 2011). The sands of the Hageland Diest member are thus interpreted to be the strong-current fill of narrow, elongate flow channels. The driving mechanism for near-simultaneous erosion and fill is argued to be continuous external sand supply by a coastal pathway under highstand conditions into a semi-enclosed embayment situated over the Campine and Hageland, and tributary to the marine Roerdal Valley Graben. The large-scale fill of this embayment is thought to have prograded under highstand conditions from NW to SE. The last stages of the embayment fill would have produced constriction of the ebb flow sections in channels superposed on drowned valleys situated at the SE side of the embayment, i.e. the present-day Hageland. Flow section constriction combined with constant tidal volumes to be drained at each falling tide must have highly reinforced the ebb currents. They cleared locally all early Diest deposits and scoured deep, elongate channels that also cut into the underlying deposits. The mostly cross-bedded Hageland Diest member represents the fill of these scour channels, associated with strong ebb currents and high lateral sand supply.

The proposed sedimentation process accommodates the fact that glauconites of the underlying Houthalen Sands may have been reworked in the Hageland Diest member. The proposed paleogeographical evolution is in agreement with the age correlation observed between the Hageland and the Wijshagen borehole in Limburg, both situated in the DN8 biochron, and the similar heavy mineral content: both locations are situated at the SE side of the embayment. In the Veerle borehole, the sands of the Dessel Member hold DN8 and are overlain by the Hageland sand facies. Sedimentation of the Dessel-Deurne Sands in the part of the embayment situated over the Campine area might have played the role of the basin-scale prograding fill causing sand pressure

**Figure 10.** Sketch of middle Tortonian DN9 biochron paleogeography. The Campine Diest Formation transgression brought reworked Antwerp Sands from the NNW back to the subsiding central Campine where they became mixed with Kieseloolite quartzic deposits from the extending Rhine delta. Ma (Maaseik), Mo (Mol), A (Antwerp), Aa (Aarschot), B (Brussels), L (Leuven), H (Hasselt), G (Genk).



and flow constriction at the far side of the embayment; they may therefore have been in part synchronous with the Hageland Diest member facies development. This is compatible with the glauconite dates found in the base of the Diest Formation at Retie and Kalmthout (Table 3). In sequence stratigraphic terms, the lower part of the Campine Diest Formation that is age-correlated with the Hageland Diest member, together with the Hageland Diest member, are the prograding highstand-systems tract and, together with a basal part of the Dessel Member in the Campine which may be a remnant of the transgressive systems tract (base of Diest Formation in Retie, Kalmthout and Dessel), could represent the Tor1 sequence (Hardenbol et al., 1998) (Fig. 4).

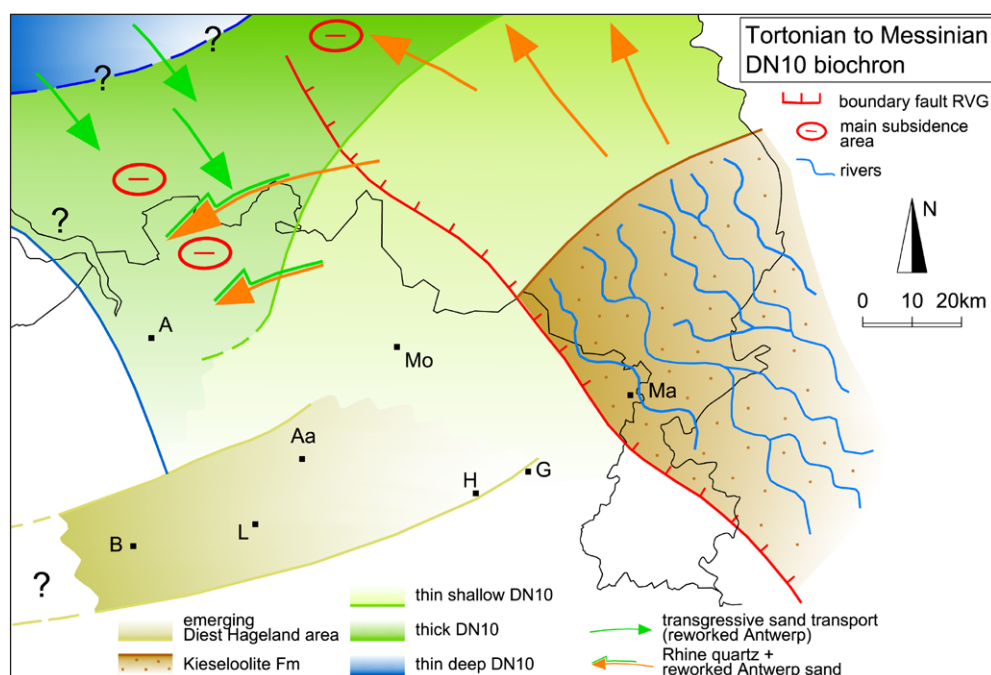
In conclusion, the character and glauconite dates of the first cycle of the Diest Formation are compatible with a semi-enclosed marine embayment fill; however, the proposed paleogeography is still speculative and the exact nature of the different facies and their geometric architecture remain to be determined in detail, when more sedimentological data become available.

A shallow iron crust developed soon after emergence of the Hageland Diest member explaining that the deposits are still preserved today as the Hageland hills.

### 6.3. Middle to late Tortonian DN9 biochron (ca 8.5 -7.5 Ma) (Fig. 10)

At the beginning of the DN9 biochron two important paleogeographic changes occurred in the Campine Basin. First, from the north, an important renewed transgressive pulse occurred in the strongly subsiding central Campine area (Fig. 3), bringing coarser Campine Diest Sands over the finer, calcareous Deurne-Dessel Members and some high stand systems tract basal sands of the Campine Diest member. This transgressive phase might correspond to the beginning of the Tor2 sequence (Hardenbol et al., 1998) (Fig. 4). No particular surface at the base of this new transgressive pulse has been observed, either because the information from boreholes is not suitable for its detection or because the amplitude of the sea-level low between the two sequences was too small to lead to significant emergence of the Campine area. The second important change was the input from the Rhine delta in the east of massive amounts of coarse-grained quartz-rich sands after the rearrangement of the Rhine river system in Germany (Fig. 10). These coarse quartz-rich sediments initially form the fluvial Inden Formation developing later

**Figure 11.** Sketch of upper Tortonian to Messinian DN10 paleogeography. The Rhine graben deposits continue to prograde northwestward and the main area of sedimentation in front of it is shifted to the western Campine area. Ma (Maaseik), Mo (Mol), A (Antwerp), Aa (Aarschot), B (Brussels), L (Leuven), H (Hasselt), G (Genk).





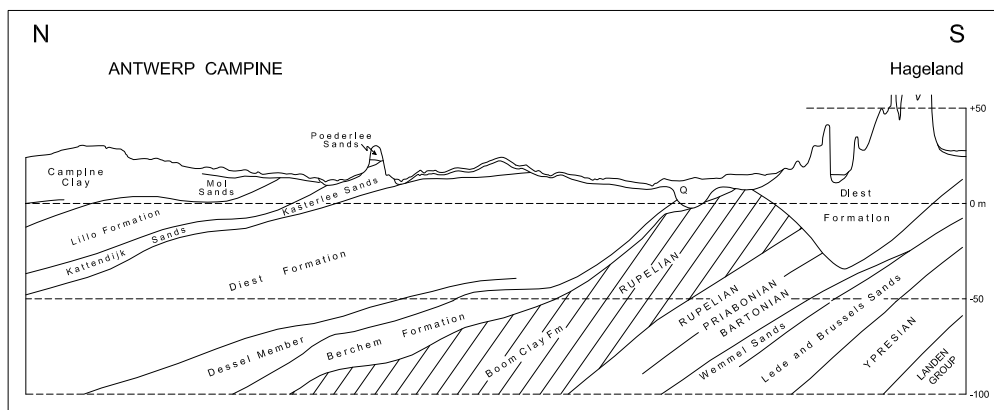


**Figure 12.** North-south cross section from the Antwerp Campine area to the Hageland area (simplified from Laga, 1975) showing the close location near each others of the north dipping Campine Diest Formation and the Hageland Diest member underlain by deep erosion. The location of the profile is shown on Fig. 1.

into the Kieseloolite Formation, a gravelly braided river facies (Schäfer et al., 2004; Wong et al., 2007). The glauconite dates of the Campine Diest member are interpreted to indicate the marine invasion of masses of reworked Antwerp Sands, probably from the area northwest of Antwerp, possibly also from some earlier eroded Antwerp Sands deposited at the rim of the graben during the end of the Serravallian river erosion. The volume of reworked sand is estimated from glauconite contents to be more than half the present Diest Formation volume. The transgressing waters swept these sands into the central Campine area where they became mixed with quartz sands delivered by the Rhine system, which progrades into the graben and spreads out over the subsiding Campine area. This may explain why, on the high-resolution seismic survey in the Campine canals (De Batist & Versteeg, 1999), oblique master beddings, observed in the eastern Campine, disappear west of the area between Mol and Geel. The seismic oblique master beddings in the east clearly overlie an irregular seismic facies as shown on the profile Bocholt-Lommel interpreted as Diest member sand overlying Dessel Member sand by De Batist & Versteeg (1999). Progradation of the delta front is indicated by the dominant southwestward to westward oriented transport directions inferred for the Campine Diest Formation from all seismic sections (Fig. 5) and by the westwards thinning of the DN9 sediments (Fig. 3). This paleogeographic model can also explain the variability of the sediments observed in core descriptions of the Campine Diest member, both coarse and finer sands occur and angular quartz grains can be quite characteristic in some intervals; also black clayey sands and lignite staining are described as in the Poppel facies. The transgression from the northwest also produced a fine-grained Dessel type facies as shown by the DN9 biozonation in some Dessel Member facies (Retie and Mol boreholes in Fig. 3). This Campine type Diest member presently ends in the south where the Hageland hilly landscape begins (see below an example in Fig. 12), suggesting that the marine realm during the DN9 biochron was bordered in the southeast by the already somewhat elevated proto-Hageland landscape that formed after the regression at the turn of DN8 and DN9 biochrons. The Hageland Diest member stands out in relief because its top was iron-cemented shortly after emergence.

#### 6.4. Latest Tortonian to early Messinian, DN10 (ca 7 Ma) biochron (Fig. 11)

Continuing from the DN9 biochron paleogeography, during the DN10 biochron the Kieseloolite Formation prograded further to the northwest in the Roer Valley Graben (Schäfer et al., 2004) and a mixture of reworked Antwerp Sands and quartz-rich Kieseloolite type sediment was deposited in the western Campine area (Fig. 3). The quartz-rich Opoeteren and Poppel facies in the top of the Diest Formation (Table 1) are probably the Diest Formation facies most influenced by the Kieseloolite type sediment. The westward filling of the subsiding Campine area continues later during the Pliocene when large masses of Pliocene glauconitic sands are deposited in the Antwerp harbour area (de Heinzelin, 1963) while quartz-rich Mol Sands, equivalent of the Kieseloolite Formation, continued to progress over the area from east to west (Fig. 13 (Buffel et al., 2001). Also Verbeek et al. (2002) and Wong et al. (2007) have documented in the northwestern part of the Roer Valley Graben in The Netherlands a low angle clinoform with an apparent dip to the southwest, interpreted by these authors as mainly Pliocene clinoforms.

## 7. Conclusions

The dating of glauconite grains from the Dessel Member, the Hageland Diest and the Campine Diest members has shown that, except for a greensand at the base of the Dessel Member, the glauconite grains are reworked. Still, the dates for the samples from the Hageland and those from the higher levels of the Campine Diest member are different. The west and central Campine samples are reworked Antwerp type Sands. Regional geological considerations indicate the Hageland samples are more influenced by reworked Houthalen Sands. The reworking is massive. The analysis allowed the distinction of two sedimentary sequences. The oldest sequence formed during biochron DN8 as transgressive sands of the Dessel-Deurne Members were deposited in a shallow semi-enclosed marine embayment area over the subsiding Campine and Hageland areas. The sedimentation of these sands continued and they filled the embayment from the north-northwest during the high-stand; this process caused flow

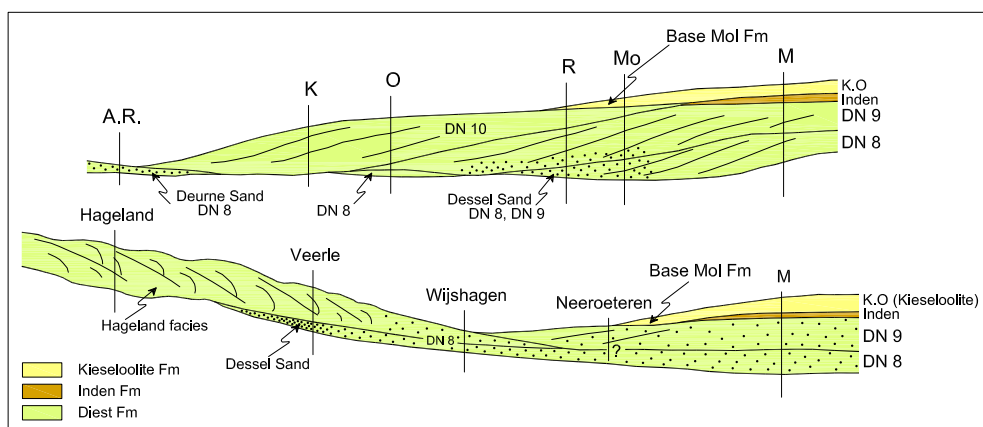


**Figure 13.** Profile sketches through the Diest Formation and the Inden and Kieseloolite Formations from west (A.R. Antwerp Rivierenhof) to the Roer Valley Graben in the east, and from the Hageland area in the southwest to the Roer Valley Graben in the northeast. The position of the boreholes used to construct the profiles and the approximate profile positions are shown in Fig. 1. Note that the base of the Mol Formation in Belgium is considered in this sketch to represent the prograding of the Kieseloolite Rhine delta sediments from the RVG to the southeast.

constriction in the bay and consequently very strong currents, deeply eroding and massively removing underlying sediments. The Hageland Diest member is the fill of these erosive valleys. In this paleogeographic model the Hageland Diest Sands are in part contemporaneous with the Dessel Sands (DN8) and with some coarser sands of the Diest member that cover the Dessel Member in parts of the transition area between the Campine area and Hageland area (Veerle borehole) or that occur laterally away from the Dessel Member (Wijshagen borehole, with dinoflagellate cyst biozone DN8) (Fig.13).

Glaucinite dates and sediment properties suggest that sands brought to the Campine area by a second transgression during the Tortonian biochron DN9 consisted of a mixing of reworked Antwerp type Sands and quartz-rich sands delivered from the Rhine delta that was filling the Lower Rhine Graben in the east. A Dessel Member facies also formed during this DN9 transgression. During biochron DN9, sediment was transported from the delta front to the west and southwest filling the subsiding central Campine and later also the western Campine during biochron DN10. This sediment transport explains the westward and southwestward clinoform dips observed on seismic sections, different from the oblique stratification dips measured in outcrops of the slightly older Hageland Diest member.

The model derived in this study has the merit of explaining most of the presently known information on the Diest Formation in a coherent geological history. Data however are too scarce and not sufficiently representative for a refined model. Therefore, the model presented in this study needs to be further tested by and adapted to new sedimentological, mineralogical, sediment-petrological, paleontological, and geochronometrical data.

## 8. Acknowledgements

NIRAS-ONDRAF and the Belgian Geological Survey are thanked for allowing access to the boreholes, help with the sampling and providing information on the boreholes. Jessica E. Raines assisted in six of the K-Ar determinations. Caroline Vandenheuvel and Jorik Van Wilderode are thanked for help with analyses. Greet Willems was of great help in drafting several versions of the figures. The reviewers are thanked for their helpful comments that led to improvement of the manuscript.

## 9. References

- Amorosi, A., Sammartino, I. & Tateo, F., 2007. Evolution patterns of glaucony maturity: a mineralogical and geochemical approach: Deep-Sea Research II, 54, 1364-1374.
- Bastin, A., 1966. Sedimentpetrologie van de Zanden van Edegem en de Zanden van Antwerpen. Het Ingenieursblad, Koninklijke Vlaamse Ingenieursvereniging, 35/17, 547-550.
- Buffel, P., Vandenberghe, N., Goolaerts, S. & Laga P., 2001. The Pliocene sediments in 4 boreholes in the Turnhout area (North-Belgium): the relationship with the Lillo and Mol Formations. Aardkundige Mededelingen, University Press Leuven, 11, 1-8.
- Dalrymple, G.B. & Lanphere, M.A., 1969. Potassium-Argon Dating. Freeman, 258p.
- Dalrymple, R.W. & Choi, K., 2007. Morphologic and facies trends through the fluvial-marine transition in tide-dominated depositional systems: A schematic framework for environmental and sequence-stratigraphic interpretation. Earth-Science Reviews, 81, 135-174.
- De Batist, M. & Versteeg, W.H., 1999. Seismic stratigraphy of the Mesozoic and Cenozoic in northern Belgium: main results of a high-resolution reflection seismic survey along rivers and canals. Geologie en Mijnbouw 77, 17-37.
- de Heinzelin J., 1963. Carte et coupe d'ensemble de la région anversoise. Mémoires Société belge de Géologie, Série IN-8° N°6, 247-248, 1pl.
- Delvaux, M., 1884. Compte rendu de l'excursion du 16 Août au Musiekberg et au Pottelberg. Annales de la Société Géologique de Belgique, 12, 74-114.
- De Man, E., Van Simaey, S., Vandenberghe, N., Harris, W.B. & Wampler, J.M., 2010. On the nature and chronostratigraphic position of the Rupelian and Chattian stratotypes in the southern North Sea Basin. Episodes, 33 (1), 3-14.
- De Meuter, F.J. & Laga, P.G., 1976. Lithostratigraphy and biostratigraphy based on benthonic foraminifera of the Neogene deposits of Northern Belgium. Bulletin Société belge de Géologie, 85(4), 133-152.
- Demyttenaere, R., 1988. De Post-Paleozoïsche geologische geschiedenis van Noord-België. Doctoraats thesis, K.U. Leuven.
- Demyttenaere, R., 1989. The Post-Paleozoic Geological History of North-Eastern Belgium. Mededelingen Koninklijke Academie Wetenschappen Letteren en Schone Kunsten van België, Klasse Wetenschappen, 51 (4), 51-81.
- de Verteuil, L. & Noris, G., 1996. Miocene dinoflagellate stratigraphy and systematics of Maryland and Virginia. Micropaleontology, Supplement 42: 1-172.
- Geets, S. & De Breuck, W., 1991. De zware-mineraleninhoud van Belgische Mesozoïsche en Cenozoïsche afzettingen. G. Neogeen. Natuurwetenschappelijk Tijdschrift (Gent) 73, 3-37.
- Gliese, J. & Hager, H., 1978. On Brown coal resources in the Lower Rhine embayment (West Germany). Geologie en Mijnbouw 57 (4), 517-525.
- Gulincx, M., 1962. Essai d'une Carte géologique de la Campine. Etat de nos connaissances sur la nature des terrains néogènes recoupés par sondages. In de Heinzelin J. & Tavernier R., Symposium sur la stratigraphie du Néogène nordique. Mémoires Société Géologique belge de Géologie, 6, 30-39.
- Gulincx, M., 1964. Boring te Neeroeteren (Groeve Knippenberg) 64W-234. Archives Belgian Geological Survey, Brussels.
- Gulincx, M., 1973. Geological cross section W-E Boom-Beringen-Opoeteren. Archives Belgian Geological Survey, Brussels.
- Gullentops F., 1957. L'origine des collines du Hageland. Bulletin Société belge de Géologie, LXVI, 81-85.
- Gullentops F., 1963. Etude de divers facies quaternaires et tertiaires dans le Nord et l'Est de la Belgique. Excursion O-P, 6e Congrès International de Sédimentologie, Belgique et Pays-Bas, p7.
- Gullentops, F., 1988. Neogene. In Herbosch A. (ed.), I.A.S. 9th European Regional Meeting, Excursion Guidebook Leuven-Belgium, Sept. 1988, Belgian Geological Survey, Brussels, 226 & 255-260.
- Gullentops, F. & Huyghebaert, L., 1999. A profile through the Pliocene of Northern Kempen, Belgium. Aardkundige Mededelingen, University Press Leuven, 9, 191-202.
- Hardenbol, J., Thierry, J., Farley, M.B., Jacquin, T., de Graciansky P.-C. & Vail, P.R., 1998. Mesozoic and Cenozoic sequence chronostratigraphic framework of European Basins. In de Graciansky P.-C., Hardenbol J., Jacquin T., Vail P.R. (eds) Mesozoic and Cenozoic Sequence Stratigraphy of European Basins SEPM (Society for Sedimentary Geology) Special Publication 60, 3-14 + 8 charts.
- Harris, W.B., 1975. Stratigraphy, petrology, and radiometric age (Upper Cretaceous) of the Rocky Point Member, Pee Dee Formation, North Carolina (PhD dissertation): University of North Carolina, Chapel Hill, 190 p.
- Harris, W. B., & Bottino, M. L., 1974. Rb-Sr study of Cretaceous lobate glauconite pellets, North Carolina: Geological Society of America, Bulletin, v. 85, 1475-1478.
- Hilgen, F.J., Lourens, L.J. & Van Dam, J.A., 2012. The Neogene Period. In Gradstein, F.M., Ogg, J.G., Schmitz, M.D. & Ogg, G.M. (eds) The Geological Time Scale 2012, Elsevier BV, 923-978.
- Hooyberghs, H. & Moorkens, T., 2005. Biostratigraphic study of the 'Middelares Hospital' outcrop section in the Deurne Sand Member (upper Miocene, Belgium) as based on foraminifera. Abhandlungen Neues Jahrbuch Geologie und Paläontologie 237(1), 5-28.
- Houbolt, J.J.H.C., 1982. A comparison of recent shallow marine tidal sand ridges with Miocene sand ridges in Belgium. In Scraton, R.A. and Talwani, J.M., The Ocean Floor, John Wiley & Sons Ltd., 69-80.
- Houthuys, R., 2011. A sedimentary model of the Brussels sands, Eocene, Belgium. Geologica Belgica, 14, 55-74.
- Houthuys, R., in review. A reinterpretation of the Neogene emersion of central-Belgium based on the sedimentary environment of the Diest Formation and the origin of the drainage pattern. Geologica Belgica.
- Keppens, E., 1981. Onderzoek van het glauconiet als geochronometer voor de Rb-Sr dateringsmethode: toepassing op ceno- en mesozoïsche afzettingen in Belgische en naburige bekkens met het oog op de verbetering van de absolute tijdschaal. Doctoraatsproefschrift, Geologie, VUB Brussel, België.
- Keppens, E. & Pasteels, P., 1982. A comparison of rubidium-strontium and potassium-argon apparent ages on glauconies. In Odin, G.S. (ed.), Numerical dating in stratigraphy, John Wiley and Sons, 225-243.
- Keppens, E., Clauer, N., & Odin, G.S., 1984. Inheritance of radiogenic <sup>87</sup>Sr and <sup>40</sup>Ar in glauconites: Terra Cognita, 4, 41-42.
- Kuhlmann, G., 2004. High resolution stratigraphy and paleoenvironmental changes in the southern North Sea during the Neogene. Geologica Ultraetina 245, 205p.

- Labat, S., Gedeon, M., Beerten, K. & Maes, T., 2011. Dessel-5 borehole: technical aspects and hydrogeological investigations. External report SCK-CEN-ER-151 11/Slap-1, 39p.
- Laga, P., 1973. The Neogene deposits of Belgium. Guide book for the Field Meeting of the Geologists Association, London. Belgian Geological Survey, Brussels.
- Laga, P., 1975. Geologisch Profiel Meerle-Olen-Houwaert. PGL 75/104/1 Archives Belgian geological Survey, Brussels
- Laga, P., 1982. Les dépôts Néogènes de la Belgique. Guide d'excursion tome I: Groupe Français d'étude du Néogène 28-30 Avril 1982. Service Géologique de Belgique, Bruxelles.
- Laga, P. & Notebaert, K., 1981. Boring Weelde 8E 133. Archives Belgian Geological Survey, Brussels.
- Louwyse, S., 2000. Dinoflagellate cysts and acritarchs from the Miocene Zonderschot Sands, Northern Belgium: stratigraphic significance and correlation with contiguous areas. *Geologica Belgica* 3, 55-65.
- Louwyse, S., 2002. Dinoflagellate cyst biostratigraphy of the Upper Miocene Deurne Sands (Diest Formation) of northern Belgium, southern North Sea Basin. *Geological Journal* 37, 55-67.
- Louwyse, S. & Laga P., 1998. Dinoflagellate cysts of the shallow marine Neogene succession in the Kalmthout well, northern Belgium. *Bulletin Geological Society of Denmark*, 45, 73-86.
- Louwyse S. & Laga P. 2005. The early and Middle Miocene transgression at the southern border of the North Sea Basin (northern Belgium). *Geological Journal* 40, 441-456.
- Louwyse, S. & Laga, P., 2008. Dinoflagellate cyst stratigraphy and palaeoenvironment of the marginal marine Middle and Upper Miocene of the eastern Campine area, northern Belgium (southern North Sea Basin). *Geological Journal* 43, 75-94.
- Louwyse, S. & De Schepper, S., 2010. The Mio-Pliocene hiatus in the southern North Sea Basin (northern Belgium) revealed by dinoflagellate cysts. *Geological Magazine* 147, 760-776.
- Louwyse, S., De Coninck, J. & Verniers, J., 1999. Dinoflagellate cyst stratigraphy and depositional history of Miocene and Lower Pliocene formations in northern Belgium (southern North Sea Basin). *Geologie en Mijnbouw*, 78, 31-46.
- Louwyse, S., De Coninck, J. & Verniers, J., 2000. Shallow marine Lower and Middle Miocene deposits at the southern margin of the North Sea Basin (northern Belgium): dinoflagellate cyst biostratigraphy and depositional history. *Geological Magazine* 137, 381-393.
- Louwyse, S., De Schepper, S., Laga, P. & Vandenberghe, N., 2007. The Upper Miocene of the southern North Sea Basin (northern Belgium): a paleoenvironmental and stratigraphic reconstruction using dinoflagellate cysts. *Geological Magazine* 144, 33-52.
- Matthijs, J., Buffel, P. & Leroi, S., 2003. Geologische dwarsprofielen doorheen het Tertiair in Vlaanderen Schaal 1:100.000 - Technische Toelichting. Geological Service Company bvba (GCS) in opdracht van het Ministerie van de Vlaamse Gemeenschap - Afdeling Natuurlijke Rijkdommen en Energie (<http://dov.vlaanderen.be>)
- Matthijs, J., Lanckacker, T., De Koninck, R., Deckers, J., Lagrou, D. & Broothaers, M. 2013. Geologisch 3D lagenmodel van Vlaanderen en het Brussels Hoofdstedelijk Gewest – versie 2, G3Dv2. Studie uitgevoerd door VITO in opdracht van de Vlaamse overheid, Departement Leefmilieu, Natuur en Energie, Afdeling Land en Bodembescherming, Ondergrond, Natuurlijke Rijkdommen, VITO-rapport 2013/R/ETE/43.
- Odin, G.S., 1975. De glauconiarum, constitutione, origine, aetateque. Recherches sédimentologiques et géochimiques sur la genèse des glauconies actuelles et anciennes; application à la révision de l'échelle chronostratigraphique par l'analyse isotopique des formations sédimentaires d'Europe occidentale (du Jurassique supérieur au Miocene inférieur), Thèse Doctorat d'Etat, Paris, 250 p.
- Odin, G.S., 1982. Numerical dating in stratigraphy, Part 1&2. Wiley and Sons, Chichester, 1040 p.
- Odin, G.S. and Matter, A., 1981. De glauconiarum origine: Sedimentology, 28, 611-641.
- Odin, G.S., Hunziker, J.C., Keppens, E., Laga P. & Pasteels, P., 1974. Analyse radiométrique de glauconies par les méthodes au strontium et à l'argon; l'Oligo-Miocène de Belgique. *Bulletin Société belge de Géologie* 83, 35-48.
- Parfenoff, A., Pomerol, C. & Tourenq, J., 1970. Les minéraux en grains, méthodes d'étude et détermination. Masson et Cie, Éditeurs, 120 Boulevard Saint-Germain, Paris. 3-24.
- Pasteels, P., Laga, P. & Keppens, E., 1976. Essai d'application de la méthode radiométrique au strontium aux glauconies du Néogène: le problème du traitement de l'échantillon avant analyse. *Comptes Rendus Académie des Sciences, Paris*, 282 Série D, 2029-2032.
- Rasmussen, E.S. & Dybkjær, K., 2013. Patterns of Cenozoic sediment flux from western Scandinavia: discussion. *Basin Research* 25, 1-19.
- Schäfer, A., Utescher, T. & Mörs, T., 2004. Stratigraphy of the Cenozoic Lower Rhine Basin, northwestern Germany. *Newsletter on Stratigraphy*, 40, 73-110.
- Sels, O., Claes, S. & Gullentops, F., 2001. Toelichtingen bij de Geologische Kaart van België, Vlaams Gewest Kaartblad 18-10, Maaseik (en Beverbeek) 1:50000. Ministerie van de Vlaamse Gemeenschap, ANRE, Brussel, België, 50p.
- Sissingh, W., 2003. Tertiary paleogeographic and tectonostratigraphic evolution of the Rhenish Triple Junction. *Palaeogeography, Palaeoclimatology, Palaeoecology*, 196, 229-263.
- Sissingh, W., 2006. Tertiary Evolution of the West European Platform: syn-kinematic stratigraphy and palaeogeography. *Netherlands Journal of Geology/Geologie en Mijnbouw* 85, 131p, 8 enclosures.
- Steiger, R.H. & Jäger, E., 1977. Convention on the use of decay constants in geo- and cosmochronology. *Earth and Planetary Science Letters*, 36, 359-362.
- Tavernier R. & de Heinzelin J., 1962. Introduction au Néogène de la Belgique. In de Heinzelin J. et Tavernier R., Symposium sur la stratigraphie du Néogène nordique. *Mémoires Société belge de Géologie*, 6, 7-30.
- Utescher, T., Ashraf, A.R., Dreist, A., Dybkjær, K., Mosbrugger, V., Pross, J. & Wilde, V., 2012. Variability of Neogene Continental Climates in Northwest Europe. A Detailed Study Based on Microfloras. *Turkish Journal of Earth Sciences*, 21, 289-314.
- Van Calster P., 1960. Het sedimentatiemilieu van het Diestiaan ten noorden van Leuven. Unpublished licentiaatsthesis Geologie, K.U. Leuven, Belgium.
- Vandenberghe, N. & Mertens, J., 2013. Differentiating between tectonic and eustatic signals in the Rupelian Boom Clay cycles (Lower Oligocene, Southern North Sea Basin). *Newsletters on Stratigraphy*, 46, 3, 319-337.
- Vandenberghe, N., Laga, P., Steurbaut, E., Hardenbol, J. & Vail, P.R., 1998. Tertiary Sequence Stratigraphy at the Southern Border of the North Sea Basin in Belgium. In de Graciansky, P.C., Hardenbol, J., Jacquin, Th. & Vail, P.R. (eds), *Mesozoic and Cenozoic Sequence Stratigraphy of European Basins*. Society for Sedimentary Geology (SEPM) Special Publication, 60, 119-154.
- Vandenberghe, N., Van Simaëys, S., Steurbaut, E., Jagt, J.W.M. & Felder, P.J., 2004. Stratigraphic architecture of the Upper Cretaceous and Cenozoic along the southern border of the North Sea Basin in Belgium. *Netherlands Journal of Geosciences/Geologie en Mijnbouw* 83, 155-171.
- Vandenberghe, N., et al., 2005. Stratigraphic interpretation of the Neogene marine-continental record in the Maaseik well (49W0220) in the Roer valley Graben, NE Belgium. *Memoirs of the Geological Survey of Belgium* 52, 39p.
- van Rummelen, F.F.F.E., 1977. Bladen Zeeuwsch-Vlaanderen West en Oost. Toelichtingen bij de geologische kaart van Nederland 1:50.000, Rijks geologische Dienst, Haarlem.
- Van Vliet-Lanoë, B., et al., 2002. Palaeogeographic evolution of northwestern Europe during the Upper Cenozoic. *Geodiversitas* 24, 511-541.
- Van Vliet-Lanoë, et al., 2010. A renewed Cenozoic story of the Strait of Dover. *Annales Société Géologique du Nord* 17 (2ième série), 59-80.
- Verbeek, J.W., de Leeuw, C.S., Parker, N. & Wong, Th.E., 2002. Characterisation and correlation of Tertiary seismostratigraphic units in the Roer Valley Graben. *Netherlands Journal of Geosciences/Geologie en Mijnbouw* 81, 159-166.
- Vinken R. (ed), 1988. The Northwest European Tertiary Basin. *Geologisches Jahrbuch, Reihe A, Heft 100*.
- Wong, Th.E., de Lugt, I.R., Kuhlmann, G. & Overeem, I., 2007. Tertiary. In Wong, T., Batjes, D.A.J., de Jager J. (eds), *Geology of the Netherlands*. Royal Netherlands Academy of Arts and Sciences, 2007, 151-171.
- Zaitlin, B.A., Dalrymple, R.W. & Boyd, R., 1994. The stratigraphic organization of incised-valley systems associated with relative sea-level change. In Dalrymple, R.W., Boyd, R. & Zaitlin, B.A., (eds), *Incised-valley systems : origin and sedimentary sequences*. SEPM special publication 51, 45-60.